ELSEVIER

Quaternary Science Reviews 25 (2006) 362–389

QSR

Rogen moraine: an example of glacial reshaping of pre-existing landforms

Per Möller*

GeoBiosphere Science Centre/Quaternary Sciences, Lund University, Sölvegatan 12, SE-22362 Lund, Sweden

Received 23 May 2004; accepted 19 January 2005

Abstract

Rogen moraine is widely distributed in the core areas of the former Scandinavian and Laurentide ice sheets. It is generally agreed upon that these gently arched, ice-flow transverse ridges can be used in reconstructions of paleo-ice-flow patterns and that they indicate a melted-bed or poly-thermal basal ice regime. However, the processes of ridge generation have been contentious. This study proposes a two-stage formation of Rogen moraine, based on detailed sedimentological and structural investigations in excavated trenches in a Rogen moraine landscape in the province of Dalarna, central Sweden. Field data suggest that Rogen moraine ridges are the reshaped remains of pre-existing transverse moraine ridges, originally deposited from ice-cored moraines in an ice-marginal zone. Due to back- and down-wasting of ice-cores, inter-ridge troughs were filled with debris flow and fluvial deposits, which after landscape inversion were transformed to areas of transverse and hummocky moraines. It is proposed that this primary landscape formation occurred during an Early Weichselian deglaciation. This relict landscape was later preserved beneath cold-based Mid- to Late-Weichselian ice sheet(s), which turned wet-based during the Preboreal deglaciation phase and re-moulded the precursor landforms into Rogen moraine.

1. Introduction

Rogen moraine forms one of the most conspicuous examples of glacially sculptured landscapes. These landforms, named after Lake Rogen in Härjedalen, Sweden, where they were first described (Hoppe, 1959; Lundqvist, 1969), are typical of the core areas of former ice sheets. They cover considerable areas in central and northern parts of Sweden (Lundqvist, 1981) and the former core-areas of Laurentide ice sheets in North America, where they are often called 'ribbed moraines' (e.g. Hughes, 1964; Cowan, 1968; Aylsworth and Shilts, 1989). Rogen moraine areas, in the classical sense, are characterized by anastomosing to curved ridges and intervening troughs, all lying transverse to former ice-flow direction. A characteristic feature, at least in some areas, is the gradual up- and down-ice flow-direction transition to drumlins (Lundqvist, 1969, 1989), sometimes with streamlined moraine hummocks in between the end-member landforms. Equally characteristic is a non-transitional lateral shift to streamlined terrain (cf. Aylsworth and Shilts, 1989).

Few glacial landforms have been subjected to such change in their genetic interpretation as Rogen moraine. At first they were regarded as end moraines (Frödin, 1925), but were later suggested to be supraglacial, stagnant ice features deposited in open crevasses (Lundqvist, 1943, 1958). Contrary to this, Granlund (1943) suggested that deposition took place in basal crevasses, into which till was squeezed due to ice overburden pressure. Formation by active-ice processes was suggested by Cowan (1968), Lundqvist (1969) and Sugden and John (1976, p. 245), further advanced by Shaw (1979), Bouchard (1989) and Aylsworth and Shilts (1989). The latter authors suggested a two-phase formation of Rogen moraine, with an active phase during which there was a near-base folding (Shaw, 1979)

*Tel.: +46 46 2229888; fax: +46 46 2224419.
E-mail address: per.moller@geol.lu.se.

0277-3791/$ - see front matter © 2005 Elsevier Ltd. All rights reserved.
doi:10.1016/j.quascirev.2005.01.011

or stacking (Bouchard, 1989; Aylsworth and Shilts, 1989) of debris-rich ice, followed by stagnation and passive, mainly subglacial, melt-out of the differentially distributed debris-rich ice into Rogen ridges. The studies by Shaw (1979) and Bouchard (1989) are so far the only ones based on more comprehensive sedimentological and structural investigations. For a more comprehensive review of previous studies on Rogen moraine, see Lundqvist (1989) and Hättestrand and Kleman (1999).

This wide array of theories on Rogen moraine formation and the large differences observed in the type of internal sediments—including tills, interpreted to be lodgement till, melt-out till and flow till, and glaciofluvial sediments—led Lundqvist (1989), after a thorough review of Rogen moraine properties, to propose a two-step formation of Rogen moraine. He discussed the concept of both steps taking place within the same glacial cycle as well as the possibility that the sediments were deposited during an older glacial event and then later re-shaped into Rogen moraine during a later glacier advance. Lundqvist (1989) favoured the latter possibility, which indicates that Rogen moraine was formed by the remoulding of pre-existing sediments/landforms. More recently, Lundqvist (1997) further stressed the two-step model but offered no new sedimentological or structural data supporting this view.

A new model of ribbed-moraine formation (into which Rogen moraines sensu Lundqvist (1989) are incorporated) has been proposed by Hättestrand (1997a, b), Hättestrand and Kleman (1999) and Kleman and Hättestrand (1999). This model advocates subglacial fracturing and horizontal extension of frozen, pre-existing subglacial sediments. During deglaciation, the upper portion of the subglacial sediment remains frozen but overlies thawed sediment. The horizontal boundary between these is called the Phase Change Surface (PCS) and represents the location of sliding and extension. As the PCS rises during ice retreat, a threshold is crossed where basal shear stress allows fracturing of the frozen layer and extension. The fractured fragments of the frozen bed form the Rogen ridges, and may be slightly remoulded.

Lundqvist (1969) pointed out the spatial connections between drumlins and Rogen moraine, in that he saw a gradual change from typical Rogen moraine into barchan-like mounds ending up in drumlins. This should occur along a paleo-flowline and with the Rogen moraine situated in depressions and the drumlins on higher ground. This interconnection between drumlins and Rogen moraine was even further advocated by Boulton (1987), who regarded them as end-member landforms in a subglacial bedform system. The subglacial bedform concept is now rapidly evolving with the introduction of 'space' geomorphology, using satellite images and/or Digital Elevation Model (DEM) data to map ice-flow-parallel and ice-flow-transverse landforms, especially so for the recently 'discovered' Rogen/ribbed moraine in Ireland (Knight and McCabe, 1997; McCabe et al., 1998, 1999; Knight et al., 1999; Clark and Meehan, 2001).

The Irish 'Rogen moraine' is puzzling, as the ridges show characteristics that differ quite markedly from what in Scandinavia is identified as Rogen moraine, and also from the ribbed moraine form-group (Hättestrand, 1997a, b). According to Knight and McCabe (1997) "a continuum of ridge morphological types exists between end-members of intact ridges and streamlined ridges", the 'intact ridges' being interpreted as Rogen moraine generated early during the last deglaciation phase and then to varying degrees modified due to drumlinization. However, what is presented as 'intact/unmodified' Rogen ridges (e.g. Knight and McCabe, 1997, Fig. 4; Knight et al., 1999, Fig. 3) show no planforms of typical Rogen moraine, whereas ridges that possibly do resemble Rogen moraine are termed 'remoulded/overprinted' Rogen ridges. The formation of the original ridges is poorly explained, with only a general reference to Hättestrand's (1997a) fracturing model. However, it is difficult to accept that the Hättestrand model applies to these ridges, because many of them contain bedrock cores (Knight et al., 1999, Fig. 3).

Based on DEM observations, Clark and Meehan (2001) describe transverse moraines, termed ribbed moraine, from central north Ireland, which includes the areas described by Knight and McCabe (1997) and Knight et al. (1999). Perhaps due to the different mapping method, their ridge patterns resemble more the Scandinavian ribbed/Rogen moraine. A very large difference, however, is the size range and topographic/spatial distribution. The Irish ribbed moraine, as described by Clark and Meehan (2001), show a much greater size range and maximum size than Scandinavian forms, being up to 16 km long and 1.1 km wide! The Irish forms also show a continuous cover over extremely large areas and are not—as is more or less always the case in Scandinavia—confined to low-lying areas. The interrelations with superimposed drumlins and drumlins down ice lead them to the conclusion that "generation of the two bedform suites is highly related, with the drumlinization closely following production of the ribbed moraine". With respect to formative processes, it is by Clark and Meehan (2001) suggested that a 'subglacially controlled bedforming switch' favours ribbed bedform formation over an arbitrary length of time, and that the Hättestrand (1997a) fracturing model would fit well for the main part of their identified ribbed moraine sets, but sometimes not. In summary, the investigators of the Irish Rogen/ribbed moraine suggest that the primary formation of transverse-to-ice-flow ridges is, both in time and space, closely connected to the formation of parallel-to-ice-flow streamlined terrain, usually with a late-stage overprint of the latter on the

former. The two bedform types are thus in this context regarded as forming a subglacial bedform system.

The last ca 20 years have, as discussed above, produced papers that show a wide variety of moraine ridges that are interpreted to have formed subglacially and that are roughly perpendicular to ice flow. These include 'classic Rogen moraine', 'blocky ribbed moraine', 'fish-scale ribbed moraine' and 'dune-shape ribbed moraine' (Aylsworth and Shilts, 1989) or Rogen moraine, 'hummocky ribbed moraine', 'Blattnick moraine' and 'minor ribbed moraine' (Hättestrand, 1997a, b). It is not clear whether or not these features are mere variations on the same theme (they are all ribbed moraine) or that each has a particular formation history. The Hättestrand group (Hättestrand, 1997a, b) has decided to take the former stand-point, that all of these are merely different types of ribbed moraine with a common origin. Their theory of formation (see above) thus implies that the content of the moraines is unimportant, i.e. the ridges are going to contain simply whatever subglacial sediment was available. Therefore, to look inside the ridges is not profitable or helpful. However, I believe that internal composition is still important. For example, a recent study (Lindén and Möller, in prep.) of Niemisel moraine (Lundqvist, 1981) in northern Sweden suggests widespread melted and deforming bed conditions during formation and a very active compressional build-up of individual transverse ridges by means of folding and thrust stacking of the subglacial bed, combined with lee-side cavity deposition of glaciofluvial and gravity-flow sediments. These ridges are thus composed of sediment that clearly is coeval with the moraine form. However, Hättestrand (1997a) consider these forms to be merely another variant of ribbed moraine. I conclude that these formations are potentially distinct from each other, and that ribbed moraine as a class is polygenetic (e.g. Kurimo, 1980). Therefore it is important to continue studies on internal composition to infer ribbed-moraine genesis.

To address the unsolved question on how Rogen moraine sensu stricto is formed, a study area with extremely well-developed moraines of classic Rogen shape was chosen. These are located in the Indån valley northwest of Lake Orsasjön in the province of Dalarna (Fig. 1), central Sweden, and within the southernmost fringe of Rogen (ribbed) moraine distribution in Sweden (cf. Hättestrand, 1997b). A large problem in Rogen moraine research is the lack of well-documented sedimentological and structural data from large exposures; most studies are based on geomorphological data and information from small exposures. The project strategy was to execute comprehensive studies of sedimentary and structural properties of the moraines in large excavated sections, opened up both in mid-ridge and ridge-end (horn) positions.

2. Methods

Geomorphic mapping of moraines was conducted from aerial photographs, both from black and white (1:30,000 scale) and false-colour infrared photographs (1:60,000 scale), combined with field mapping. Sedimentological investigations on Rogen moraine were carried out in two excavated trenches (the Eggling and Kipholstjärnen sites; Fig. 1d). Lithologic units were recognized on the basis of lithofacies classification (Table 1). The boundaries between lithofacies units and their internal structures, as well as tectonic structures, were measured and documented at a scale of 1:25. Sediment samples were taken for grain-size and lithologic analysis of diamict units, which often showed different rock provenances. The lithologic analyses were carried out on gravel grades (5.6–11.2 mm) and the number of counted grains per sample usually varied between 150 and 900 grains, although most samples had over 500 grains. Clast fabric analyses were carried out on prolate pebbles excavated from horizontal benches dug into the section walls. These benches usually measured 50×30 cm in the horizontal plane and never exceeded a vertical sampling depth of 20 cm. Each fabric set comprises 30 particles with an a-axis between 3 and 12 cm; only particles with an a/b-axis ratio of $\geqslant 2.0$ were accepted. The orientation data were statistically evaluated according to the eigenvalue method of Mark (1973) and graphically manipulated with StereoNet© for Windows.

3. General geology and geomorphology of the study area

The study area is situated within the porphyry and granite region of central Dalarna (Hjelmqvist, 1966) with rocks of sub-Jotnian to Jotnian age (ca 1.6–1.2 Ga). The basement is composed of different kinds of Dala granites, porphyrites, porphyries of varying composition and Digerberg tuff, sandstone and conglomerate. Further to the west there are large intrusives of Öje diabase. All these rock types occur as clasts in the till but, with highly differing frequencies.

The study area is situated just west of the large Siljan impact structure. This Devonian impact structure has a central granite shield area with highly displaced Silurian to Ordovician sedimentary rocks along its perimeter. The margin hosts a ring of lakes—Lake Orsasjön, Lake Siljan, Lake Skattungen—and, between them, large areas with glaciofluvial delta and sandur deposits (Fig. 1b), which are at or above the highest shoreline of the Ancylus Lake (ca 210 m a.s.l.; Nordell, 1984). The central granite shield is covered by till that was drumlinized by ice flowing SSE. The hilly terrain north and west of the impact structure reaches elevations of 400–500 m and is dissected by a series of NW–SE-trending river valleys. Some of these valleys host

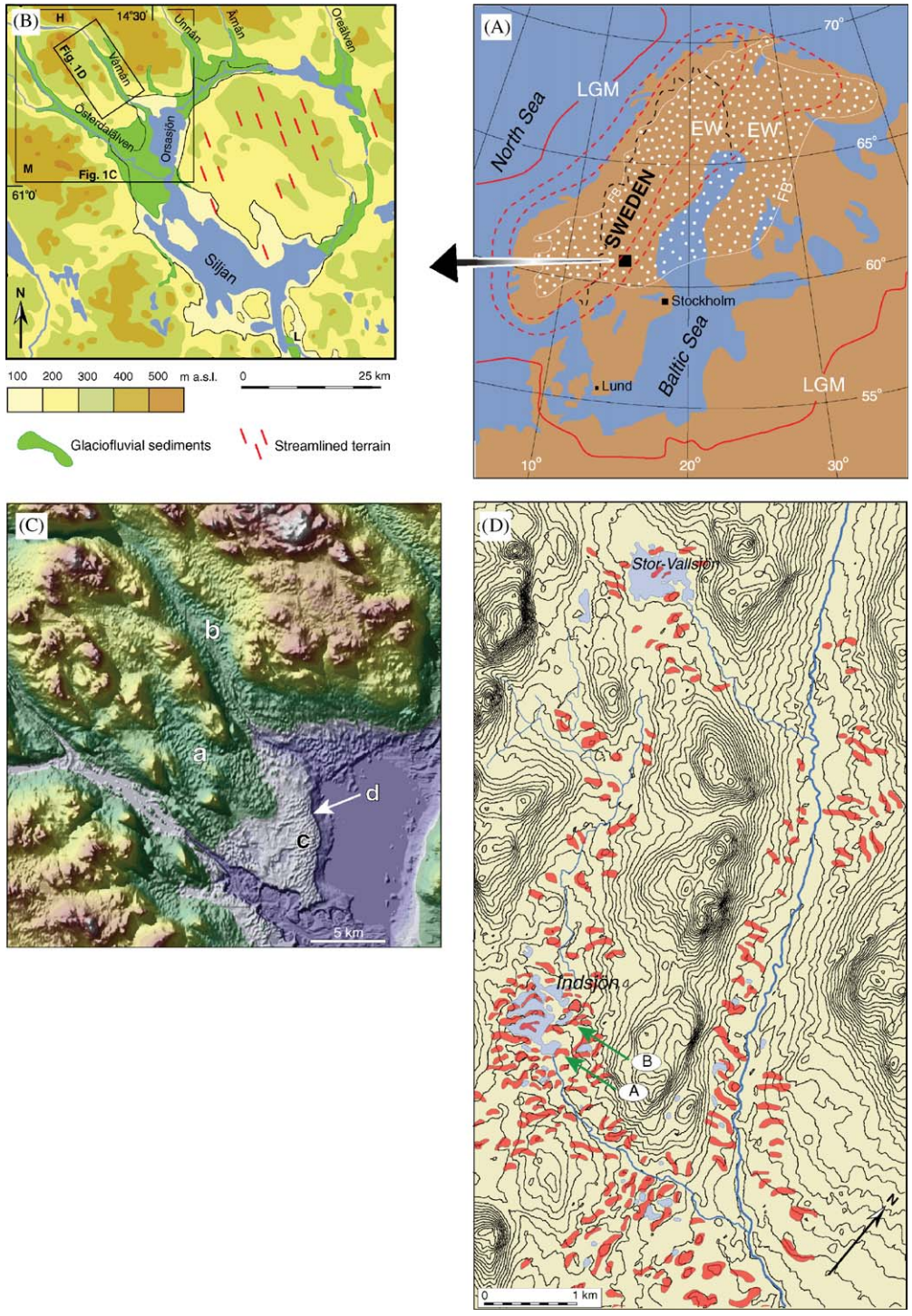

Fig. 1. Overview maps. (A) Fennoscandia with schematic ice-sheet outlines for Late Weichselian maximum (LGM) and Early Weichselian (EW), adopted from Kleman et al. (1997). Note the west-centred EW ice-sheet with its possible isotope stage 5d maximum distribution and a recessional stage (Kleman et al., 1997). White-dotted area within boundary marked FB shows the minimum extent of frozen-bed conditions during LGM according to Kleman et al. (1999). (B) Topography within and around the Siljan impact structure and main distribution of glaciofluvial sediments and streamlined terrain. Areas above the highest shoreline, ca 210 m a.s.l., are roughly delimited by the black 200 m contour. Abbreviations for places named in text: M = Myckelsjön area, L = Leksand, H = Hykjeberg. (C) Shaded relief map constructed from DEM data (for location, see b). The highest shoreline, formed by the Ancylus Lake, is marked with colour change from blue/grey to green. a = Rogen moraine in the Indor valley; b = Rogen moraine in the Vånån valley; c = eolian dunes on the Mora glaciofluvial delta; d = shoreline of ancient Lake Siljan (at ca 185 m a.s.l.) before drainage to present level due to erosion in threshold at Leksand (L in b). (D) Map of the Indån and Vånån river valleys (b for location), showing the spatial distribution of moraine ridges (planform in red). Green arrow marked A = the Eggling moraine; B = the Kipholstjärnen moraine.

Table 1
Lithofacies codes (1st, 2nd and 3d order code system) and their descriptions as used in this work (basic system according to Eyles et al. (1983), modified by Möller, 1987)

Lithofacies code	Lithofacies type description: grain size, grain support system, internal structures
D(G/S/Si/C)	Diamicton, gravelly, sandy, silty or clayey. One or more grain-size code letters within brackets
D( )mm	Diamicton, matrix-supported, massive
D( )ms	Diamicton, matrix-supported, stratified
Co- -	Cobbles, as below
D( )mm(ng)	Diamicton, matrix-supported, massive, normally graded
D( )mm(ig)	Diamicton, matrix-supported, massive, inversely graded
D( )mm (ing)	Diamicton, matrix-supported, massive, inverse to normally graded
Gmm	Gravel, matrix-supported, massive
Gcm	Gravel, clast-supported, massive
Gc(ng)	Gravel, clast-supported, normally graded
Gc(ig)	Gravel, clast-supported, inversely graded
Sm	Sand, massive
Sm(ng)	Sand, massive, normally graded
Sm(ig)	Sand, inversely graded
Spp	Sand, planar parallel-laminated
Spc	Sand, planar cross-laminated
Stc	Sand, trough cross-laminated
Sr	Sand, ripple-laminated
Sl(def)	Sand, laminated, deformed
Sim	Silt, massive
Sil	Silt, laminated

esker, sandur and kame deposits, whereas others are dominated by hummocky and/or transverse moraines, the latter in places forming well-developed Rogen moraine (Fig. 1c). Ice flow directions, as shown by striae, drumlins and transverse moraines, indicate a shift from the regional SSE direction to a late-stage, more topographically constrained flow towards SE to ESE (Nordell, 1984).

The Siljan area became deglaciated during the Pre-Boreal (11,550–10,200 cal years BP). The Ancylus Lake—a fresh-water stage of the Baltic basin—followed the receding ice margin, gradually inundating the Dalälven river valley and eventually the Siljan and Orsasjön Lake basins into which lacustrine, often varved sediments were deposited. According to Fromm (1991), the Ancylus Lake reached the entrance to Lake Siljan just north of Leksand (Fig. 1b) at varve year 580 in the Swedish varved-clay time scale, which corresponds to ca 10,500–10,600 cal years before present (e.g. Cato, 1987; Björck et al., 1996; Wohlfarth, 1996).

4. Glacial geomorphology of the Indån and Vånån river valleys

The Indån valley trends predominantly NW–SE but trends in a W–E direction at the confluence with the Vånån river valley (Fig. 1d). The valley floors (225–330 m a.s.l.) are situated well above the highest shoreline. Transverse moraines are most frequent in the wider, basin-like parts of the valleys, whereas they can be totally absent in more narrow parts. At places the moraine ridges grade into hummocky moraine, usually on flatter, slightly higher ground. Transitions from transverse ridges into drumlins, a characteristic feature of Rogen moraine according to Lundqvist (1969), are not present in the Indån or Vånån valleys. However, a transition from drumlins to drumlinized hummocky moraine to Rogen moraine in the deepest parts of a valley basin can be observed in the Myckelsjön area (Fig. 1b), some 20 km to the SW.

The Rogen moraine ridges in the Indån valley are 200–700 m long, 50–200 m wide and most commonly 10–15 m high, though they can be up to 30 m high. Usually the distal (down-ice) side of the ridges is steeper than the proximal side. Crescent-shaped forms are most prominent in the central parts of wider valley segments. The most conspicuous ridges are situated within the Indsjön Lake, where a set of moraines form segmented, boomerang-shaped islands and peninsulas (Figs. 2 and 3). In narrow valley segments or along the lateral parts of the wider valleys, only that part of the transverse ridge that points towards the central valley axis is curved down-valley, whereas the other end of the ridge is straight and/or disappears indistinctly into the valley side slope. The transverse nature of the moraine ridges is strongly coupled to topography-controlled ice flow and not the regional ice-flow direction as manifested by striae directions on bedrock heights. This is shown in NE–SW ridge-axis trends when the valley trends towards southeast, changing to N–S ridge-axis orientations when the valley trends towards the east (Fig. 1d).

The Rogen ridge surfaces (and likewise the troughs in between when not obscured by peat bogs and lakes) have usually an abundance of boulders, and in places these boulders—some of them up to 5 m in diameter—are arranged into more or less clast-supported boulder fields. These boulders are predominantly of one lithology; a general survey along the northeastern side of the Indån valley showed that up to 80–90% of all boulders >1 m in diameter are Digerberg conglomerate, which is the local bedrock. Moreover, these boulders are only found on the surface and were never encountered in the two excavations carried out in Rogen moraine ridges along the northeastern valley side. Along the south-western side of the Indån valley the large surface boulders contain similarly high percentages of red Dala granites and porphyry.

5. The Eggling section

The Eggling Rogen ridge is situated at the south-eastern end of Lake Indsjön (Fig. 1d), ca 200 m SW of

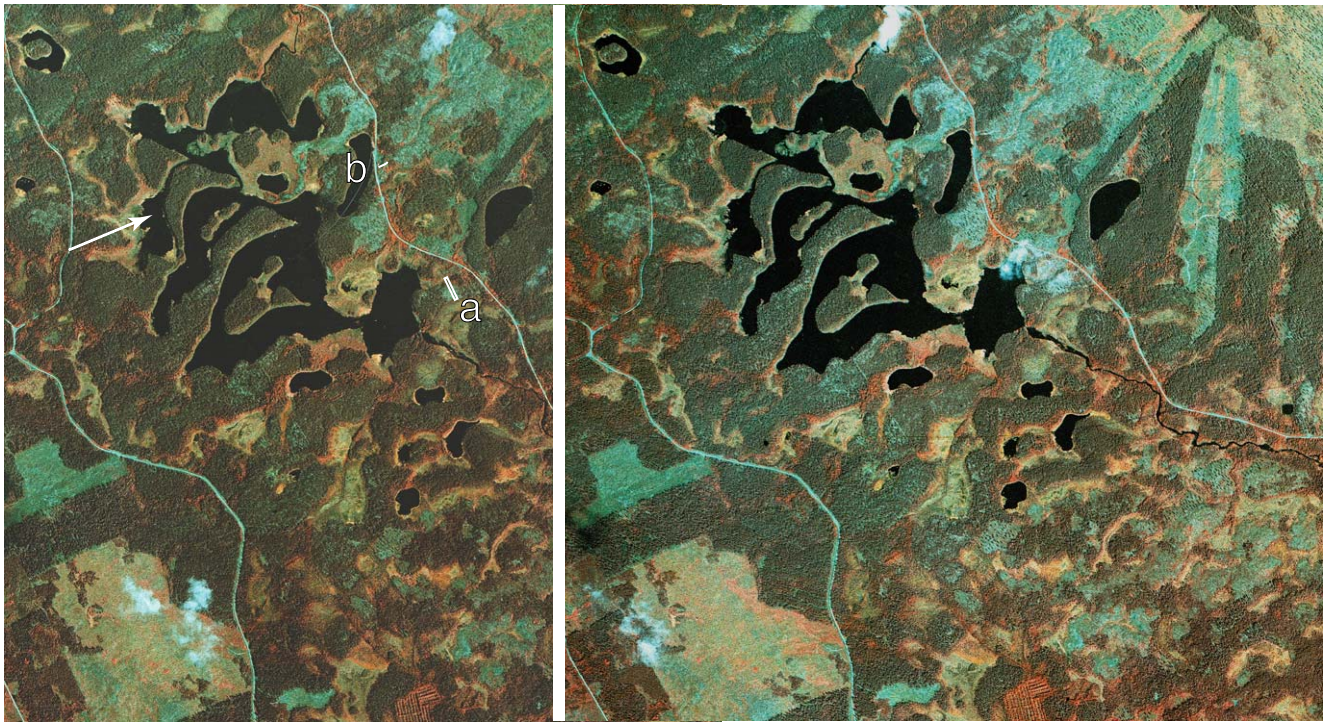

Fig. 2. Stereo-pair of the central part of the Indån valley. The white arrow indicates view direction and the left Rogen moraine in Fig. 3A. White letters a and b indicate the locations of investigated sections; (a) is a trench across the central part of a moraine ridge at Eggling, (b) is a trench across the southwestern horn of the moraine ridge at Kipholstjärnen.

Fig. 3. Highly arched and segmented Rogen moraines in the central part of the Indån valley. (A) Ice movement was from left to right; for location and view direction, see Fig. 2. (B) Same moraine ridges seen in up-glacier direction.

the small Eggling lake (Fig. 4). Like most ridges, when located in a more central part of the valley, it forms a typical Rogen planform with a pronounced and high western horn and a slightly less pronounced eastern horn (Figs. 2 and 4). The ridge rises ca 10 m above surrounding peat bogs and lakes. A bog core from 50 m outside the distal slope revealed a 5.6 m thick succession of peat and gyttja, ending in 10 cm of silt and clay. The ridge has thus a total relief of about 15 m. A section was excavated across the central part of the ridge and includes 55 m of the total width of ca 85 m (Fig. 5). The trench was excavated to the maximum capacity of the machinery (about 6.5 m), and therefore the total height of the ridge is not represented.

Macrofossils (leaves from Cyperaceae and Poaceae and one Carex seed) were wet-sieved out from a silt gyttja 10–15 cm above the base of the above-mentioned bog core. An AMS ^{14}C dating on the macrofossils gave an age of 9565 ± 95 ^{14}C years BP (11,100–10,740 cal years BP; lab no. LuA-5201), thus confirming a Pre-boreal age for the deglaciation of the area.

5.1. Sediment description

The sediments predominantly comprise reddish, gravelly-sandy to sandy-gravelly, matrix-supported and massive diamicton. Cobble- and boulder-sized clasts (boulders are up to 50 cm) are usually evenly distributed, although clast agglomerations do occur. There is a clear tendency for large boulders to be located very near or at the surface of the ridge, and boulders larger than 1 m in diameter, which are quite frequent on the surface, were never encountered within the ridge sediments. The diamicton is frequently interbedded with subhorizontal to inclined sorted sediment beds and clast horizons; if we regard the diamicton between two succeeding sorted sediment beds as one sedimentary unit, then the diamicton beds range in thickness from 20 cm up to 2 m, with a most common bed thickness between 0.5 and 1 m. A substantial number of these beds show a vertical normal clast grading, whereas a few beds carry larger clast in their tops, thus showing an inverse clast grading.

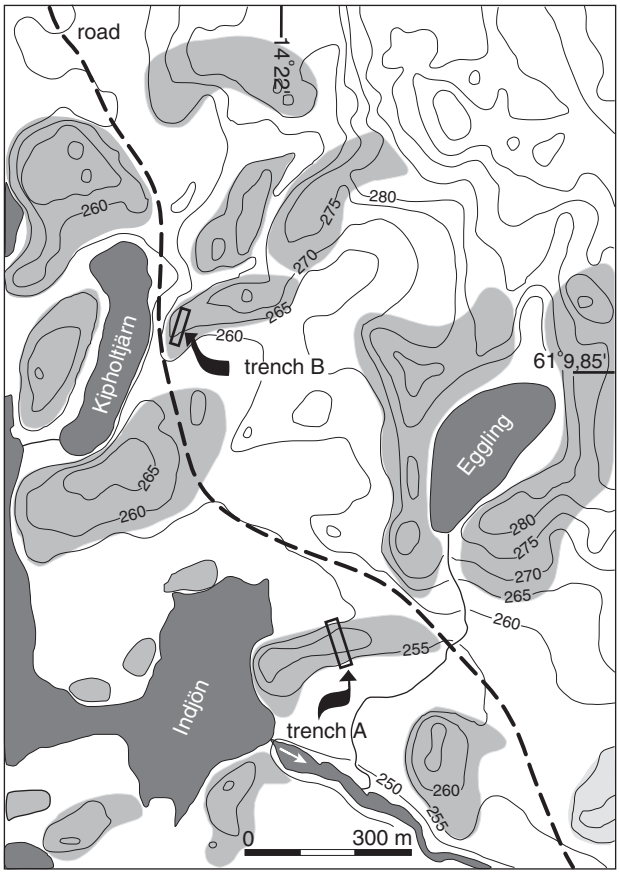

Fig. 4. Morphological map of the area surrounding the Eggling and Kipholstjärnen moraines in the Indån valley (see also Fig. 2). The outline of individual Rogen moraine ridges is shaded in grey. The positions of the trenches, cutting the moraines are marked with arrows. The Eggling trench (A) cut the moraine in mid-ridge position whereas the Kipholstjärnen trench (B) cuts the moraine along a pronounced horn pointing towards SSW (200°–20°), whereas the general trend of the ridge is 230°–50° (a 30° difference).

Clast fabric and gravel lithology analyses were carried out at six levels in diamicton beds (log d, Fig. 5). The analysed gravel grades (Fig. 6, Egg1–6) show a very high occurrence of Bredvad porphyry (27–37%) and phenocryst-rich porphyry (7–11%) throughout the section, giving the diamicton its reddish colour. The fabric analyses (Fig. 7) show weak to moderately preferred clast long-axis orientations (S_1 eigenvalues = 0.52–0.62) and highly varying V_1-axis orientations (azimuths between 266–56°). As indicated by the quite high S_2 values (0.36–0.42) and very low S_3 values, the fabric shapes can be characterized as girdle distributions (with the exception of Eggling 3, having a more clustered fabric) (Fig. 8). Calculated girdle azimuths (Fig. 7) are between 310° and 29° with dips of the girdle planes between 8° and 18°, and thus form a tighter cluster than the V_1 axes. For some data sets, the V_1 axis is nearly transverse to the girdle-plane azimuth, for others the V_1 axis is more or less parallel to the girdle-plane azimuth.

Sorted sediment facies in the Eggling section are massive and planar parallel-laminated sand, usually forming beds 2–10 cm thick and, in the projection of the section wall, 0.5–4 m long. The beds, also in the projection of the section wall, are usually sub-horizontal, but inclined beds are not uncommon with apparent dips up to 15° (excluding sediment represented by log a). Another common facies is thin (0.5–3 cm) beds of massive sandy silt, having the same dimensions and projections along the section wall as the sand beds. At places the Spp and Sm beds are connected to scours down into underlying diamict beds and/or laterally grading into clast-supported gravel beds/lags (cf. logs b, c and d). At a few places synsedimentary deformation is demonstrated with steeply inclined and/or deformed lamination, overlain with non-disturbed lamination (e.g. log e, 5–6 m). Some sand beds also show a down-bending/up-buckling lamination beneath/around boulder-sized clasts that penetrate the sediment from above. A few massive sand beds occur as quite angular, usually steeply inclined, intra-clasts within diamict beds (e.g. log b, 7 m).

Thin clast-supported gravel to cobble gravel beds occur frequently along the section, showing the same lateral and vertical projections as the sand beds (cf. log b, 10 m; log c, 8.2 m and 10.2 m; log e, 7.5 m). Sometimes they only have a thickness covering one to two clasts and could then readily be described as lag horizons (and are often laterally connected to sand beds). Sometimes they are somewhat thicker with gradational contacts or more sharp contacts to above-lying diamicton, the sharpness often due to an open-work framework. In the latter case they are easily distinguishable from the diamict bed. The thickest sorted sediment unit is found centrally in the section (log c, 11.5 m). Here a 0.5 m thick

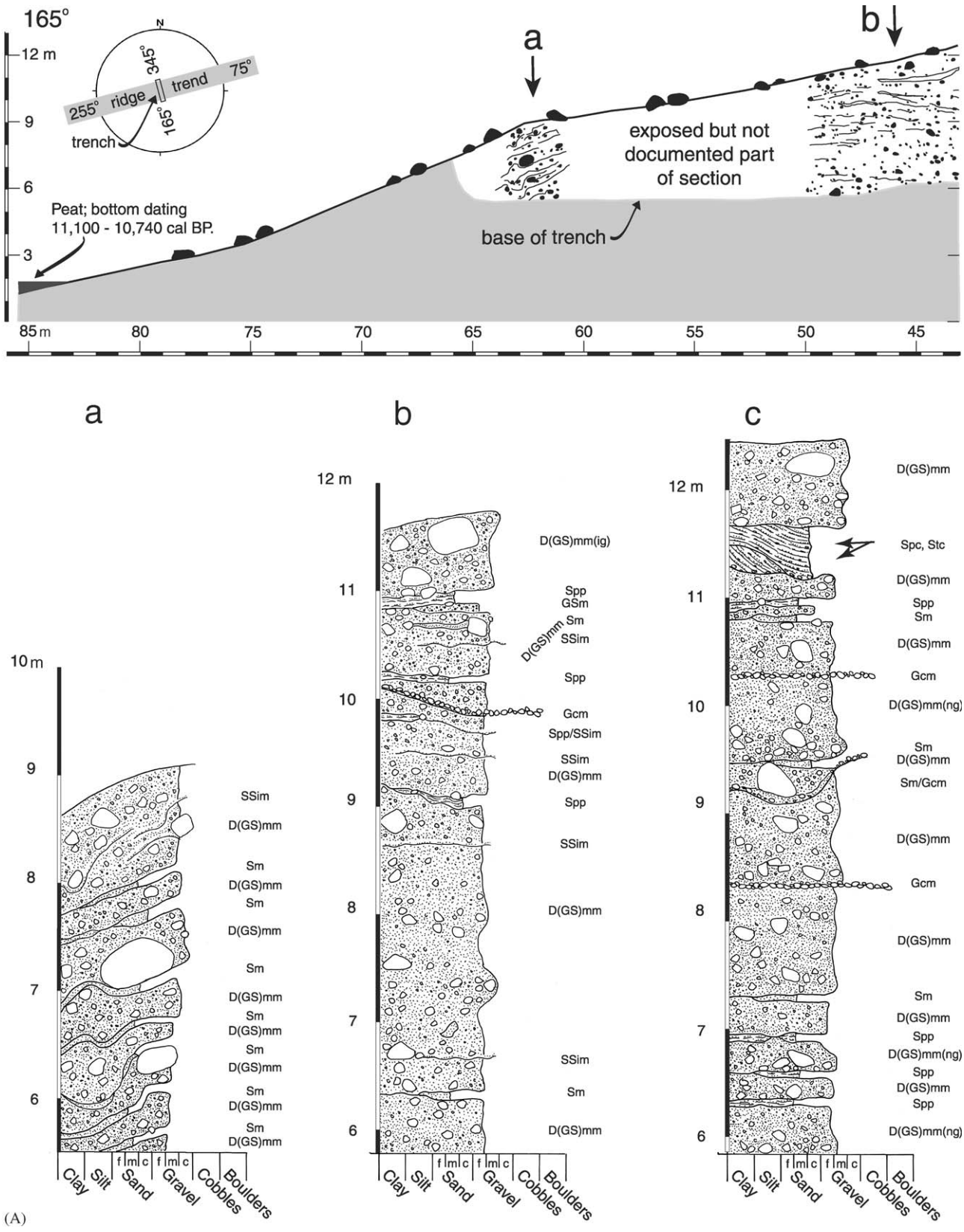

Fig. 5. Drawings of the western section wall at the Eggling site (upper panel), documented at a scale of 1:25, except for a gap between the 50 and 61 m. The section drawing is condensed to show the outline of sorted sediment beds interbedded with the predominant diamict beds and the distribution of cobbles and boulders. For a more detailed presentation, vertical facies changes are shown as six representative logs (a–f, lower panel) from specific locations along the Eggling trench section. Lithofacies codes on the logs are according to Table 1. The stars at log d indicate the locations of six lithological and clast fabric analyses (Eggling 1–6, Figs. 6 and 7).

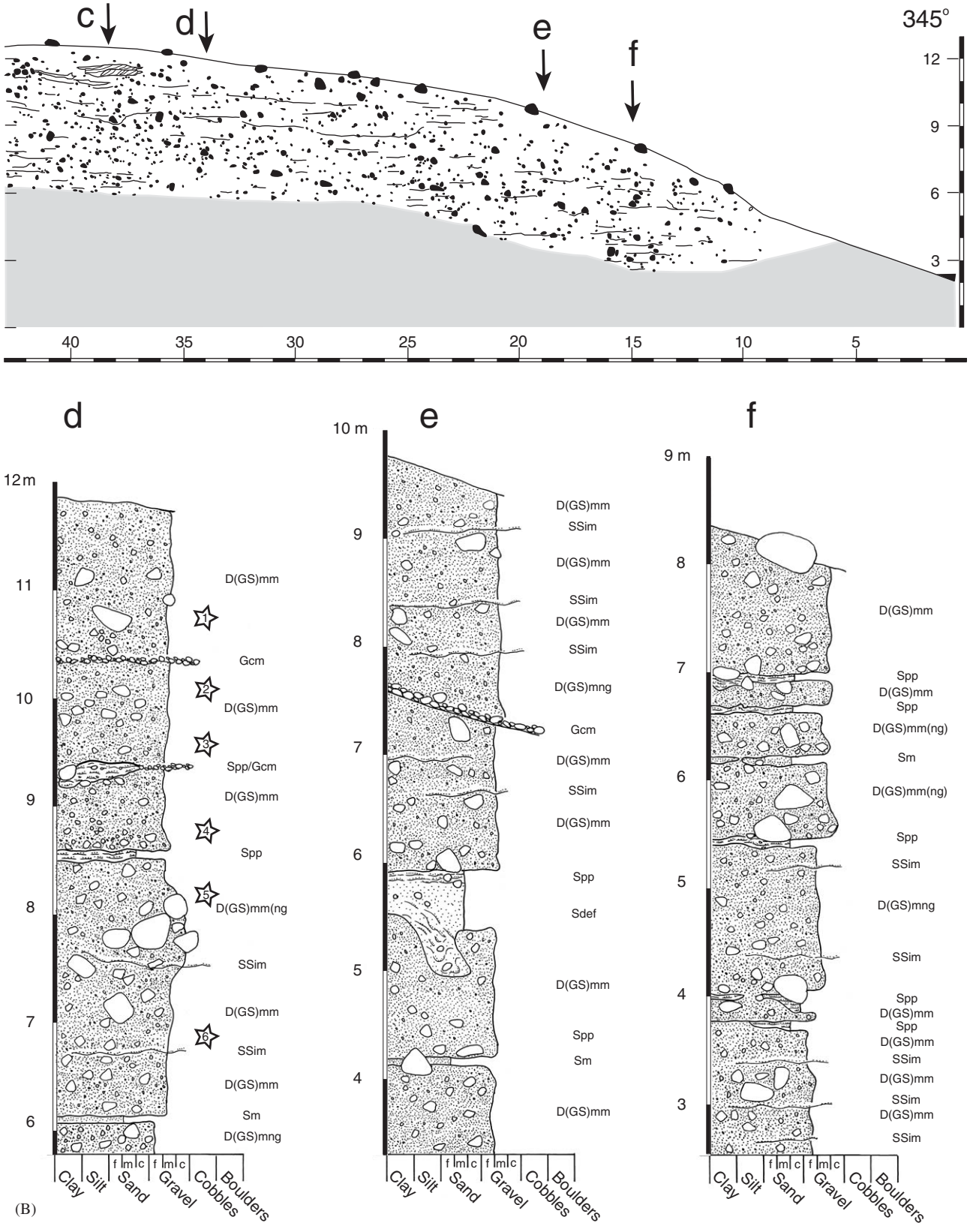

Fig. 5. (*Continued*)

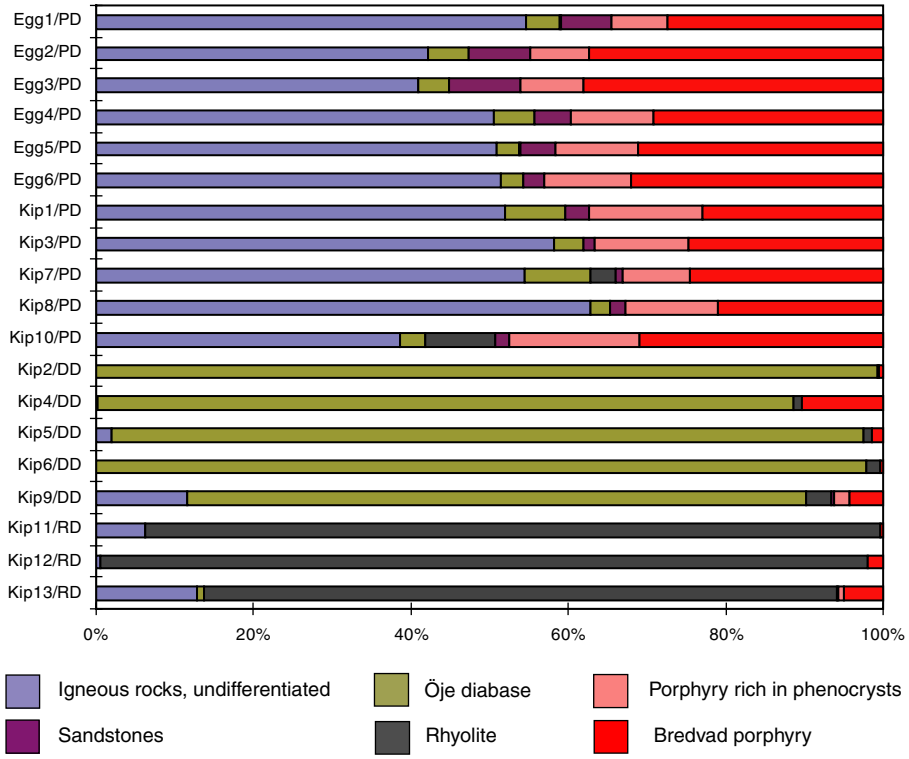

Fig. 6. Lithologic analyses of gravel grades (5.6–11.2 mm) from the Eggling (Egg1–6, se Fig. 5 for location) and Kipholstjärnen (Kip 1–13, see Fig. 9 for location) sections. Predominant lithologies give characteristic colours to the diamictons. PD = porphyry-dominated, reddish diamicton; DD = diabase-dominated, olive-green diamicton; RD = rhyolite-dominated, dark grey diamicton.

and 3 m long coset of planar and trough cross-laminated sand occurs, with an erosional base into the underlying diamicton and internally scoured bed contacts.

The sediments in log a (Fig. 5) show more or less the same facies characteristics as the rest of the section but differ in that all beds are generally inclined about 20° towards the south (i.e. the distal slope of the ridge) and at a smaller scale individual beds show an anticlinal/synclinal bending with dips of up to 70°. None of these sediments are in their original position and the sediment succession in this lateral part of the ridge thus clearly demonstrates both synsedimentary and post-depositional dislocation of the sediments. This general inclination of strata starts approximately at the 55 m mark (Fig. 5), showing increasing inclination values and deformation towards the southern end of the trench.

5.2. Genetic interpretation of sediments and depositional processes

The sediments in the Eggling section are interpreted as a stacked succession of sediment gravity-flow deposits interbedded with fluvial deposits. This is because they reveal sedimentary properties very similar to those reported from active subaerial sediment-flow depositional environments (e.g. Lawson, 1979, 1981, 1982, 1988). The internal properties of sediment-flow deposits are highly dependent on the water content and interrelated grain support mechanisms during mass movement. The dominant diamicton beds in the Eggling section are texturally similar throughout and can be interpreted as Type I low-water content flows (e.g. Lawson, 1982) with movement in a very thin basal shear zone and thus a passive transport of the overlying part of the debris flow. These types of flows will have a pebble fabric that is mostly unrelated to the flow event. However, a considerable number of the diamicton beds show a clast concentration in their lower parts (coarse-tail normal grading) indicating the development of a basal shear zone (Type II flows, Lawson, 1982), sometimes not supportive enough for the larger clasts and thus resulting in basal-zone tractional gravels. The upper part of this type of flow (the plug zone) thus resembles the Type I flow sediments. Type II flows can also form inversely graded and normally-to-inversely graded beds when the plug, due to its higher strength, carries larger clasts than is possible in the basal shear zone and this occurs in diamictons of the Eggling site, especially the upper beds in logs b and c, Fig. 5. The sporadically occurring, usually angular and inclined intra-clasts of sorted sediments are also indicative of internally immobile plug zones. With internal shearing these intra-clasts would have been disaggregated (Lawson, 1988) or deformed in the stress direction.

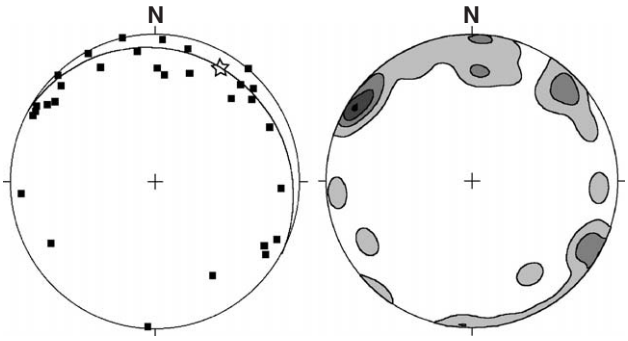

G_{az} = 29°/12°	*Eggling 1*		
n = 30	V_1 = 330°/6°	V_2 = 61°/10°	V_3 = 209°/79°
	S_1 = 0.557	S_2 = 0.404	S_3 = 0.039

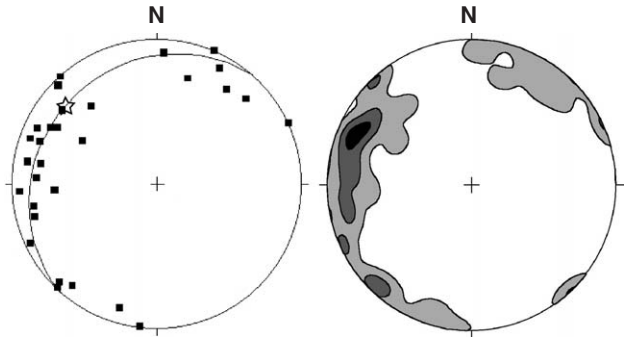

G_{az} = 310°/18°	*Eggling 4*		
n = 30	V_1 = 266°/13°	V_2 = 359°/12°	V_3 = 131°/72°
	S_1 = 0.584	S_2 = 0.384	S_3 = 0.033

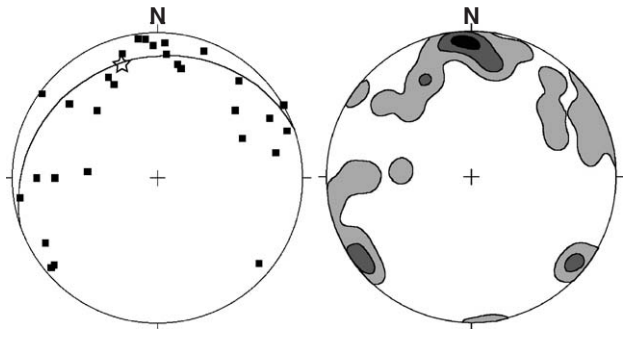

G_{az} = 340°/18°	*Eggling 2*		
n = 30	V_1 = 22°/14°	V_2 = 289°/12°	V_3 = 161°/72°
	S_1 = 0.517	S_2 = 0.411	S_3 = 0.072

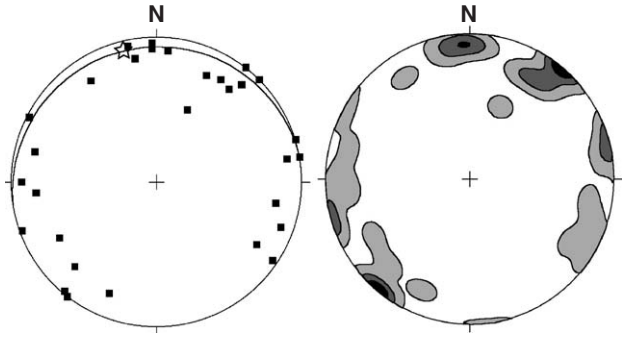

G_{az} = 350°/8°	*Eggling 5*		
n = 30	V_1 = 51°/4°	V_2 = 320°/7°	V_3 = 170°/82°
	S_1 = 0.580	S_2 = 0.361	S_3 = 0.059

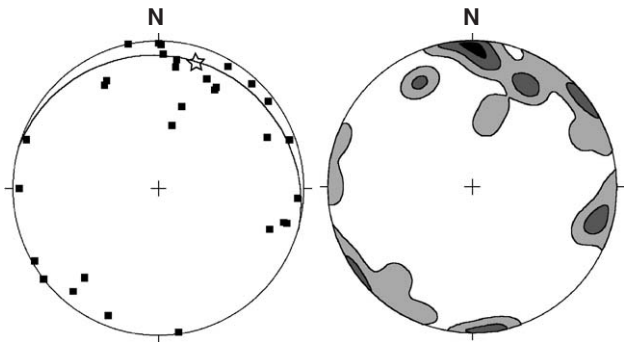

G_{az} = 14°/11°	*Eggling 3*		
n = 30	V_1 = 30°/11°	V_2 = 299°/3°	V_3 = 196°/79°
	S_1 = 0.616	S_2 = 0.321	S_3 = 0.064

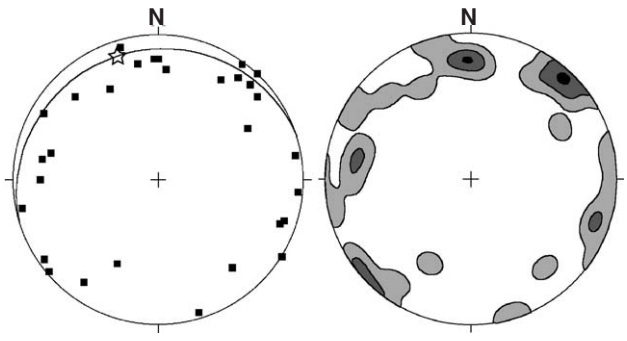

G_{az} = 341°/11°	*Eggling 6*		
n = 30	V_1 = 56°/3°	V_2 = 325°/11°	V_3 = 163°/79°
	S_1 = 0.513	S_2 = 0.419	S_3 = 0.068

Fig. 7. Schmidt equal-area, lower-hemisphere projections of clast long-axis orientations from the Eggling section (nos. 1–6; for location, see Fig. 5, log d). Both scatter plots and contoured diagrams (conventional step calculation with 1 sigma contouring interval) are included for each fabric as well as calculated eigenvectors (V_1, V_2, V_3) and normalized eigenvalues (S_1, S_2, S_3) according to Mark (1973). A best-fit plane trough the plotted data for each fabric is also drawn as a great circle; the girdle azimuth is indicated with a star in the plot and the value of the girdle azimuth (G_{az}) is shown in table.

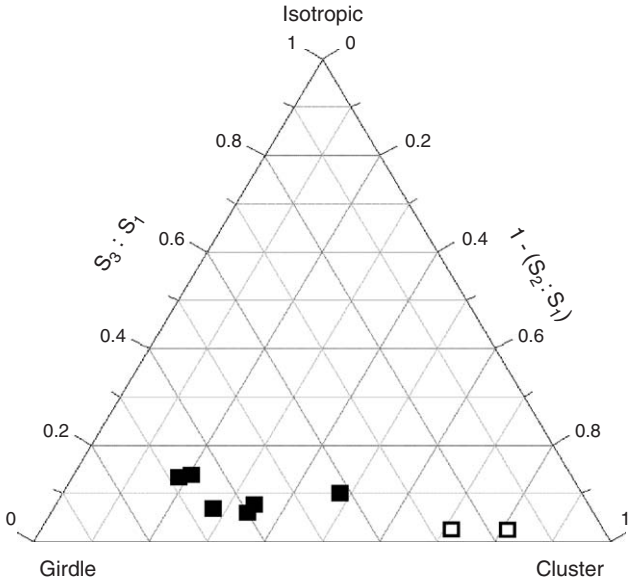

Fig. 8. Plot of the normalized eigenvalue ratios of S_3:S_1 and 1–(S_2:S_1) in a Benn ternary diagram (Benn, 1994). Filled boxes = Eggling 1–6 fabric data, open boxes = Kipholstjärnen 1–2 fabric data. Five out of six fabrics from the Eggling site show a girdle distribution, whereas the fabric shape at Kipholstjärn is strongly clustered.

Some diamict beds present at the Eggling site can also be interpreted as Type III flows (Lawson, 1982). These are more water-rich with shearing throughout and may develop, depending on grain interaction, both with an overall inverse or normal grading and thus also a pebble fabric related to the flow event. The weak to moderately preferred clast orientations with girdle distributions (Fig. 7) might indicate a fabric produced during a weak simple shear process during flow with clast axis orientations sub-paralleling the plane of flow. If this is correct the debris flows in log d (Fig. 5) indicate a sediment source in a southern sector which produced flows towards a NW to NNE-directed sector (Fig. 7: girdle azimuths between 310° and 18°).

Fluvial activity, both erosional and depositional, is widespread in the Eggling section. The erosive activity is demonstrated by numerous thin lag horizons, but also by deeper channels cut into the debris-flow units, lined with clast lags and late-stage infillings of massive to stratified sand. The largest/deepest channel can be seen in log c (Fig. 5, 11.5 m). It is infilled with cross-stratified sediments showing a westerly bar/dune migration direction. Frequently occurring silt to sand interbeds grade into thicker sand units, and these indicate an interconnected, areally distributed to channelized fluvial drainage pattern on the surfaces of stabilized debris flows. This meltwater deposited massive to planar parallel-laminated sand, at places laterally grading into erosional surfaces with lag gravel. However, all sorted sediments are probably not of fluvial origin. Some of the very thin massive sandy silty beds are interpreted as pore-water expulsion sediments, deposited on the surface of debris flows during the post-flow consolidation process (e.g. Lawson, 1988).

The overall subhorizontal to gently inclined bedding within the section, except for some minor synsedimentary deformation that can be related to local slumping and channel-wall undercutting, show that the main part of the ridge has not suffered any major post-depositional deformation. The subhorizontal stratification continues towards the proximal side of the ridge (logs e–f, Fig. 5) and is here cut at a considerable angle by the sloping ridge surface. However, the distal-side ridge sediments (log a, Fig. 5) reveal steeply tilted beds and folds that suggest a passive post-depositional lowering process in this part of the ridge. The most plausible explanation for this is melting of underlying/supporting glacier ice, likely the same ice that must be the sediment supply for the stacked sequence of sediment gravity flow deposits. As these lateral deformations do not continue towards the centre of the ridge it can be argued that the main part of the depositional basin, into which the debris-flow sediments were delivered, was not ice-floored.

An alternative interpretation for the sediments revealed in the Eggling section is that they record subglacial deforming-bed deposition. The clast agglomerations along lower contacts of diamicton beds show clast support and often an open-work framework when thicker, which is incompatible with clast pavement development at the base of a subglacial deforming bed (cf. Clark, 1991; Hicock, 1991). This is further supported by the frequent continuation of clast concentrations into stratified sorted sediment beds. Further, sorted sediment beds never show any structures indicating stress transfer from an overlying glacier interface; if these sediments should represent subglacial canal infills (cf. Alley, 1992; Clark and Walder, 1994; Walder and Fowler, 1994), then small-scale folds and thrusts would be expected to develop, at least in the upper part, where ice was coupled to the bed. Neither are there any occurrences of stretched-out sediment bodies or boudinage structures within the sequence, structures diagnostic of subglacial deformation (Benn and Evans, 1996). Clast fabric analyses do not support a deforming bed interpretation. These show low elongation index values (Benn, 1994) and relatively weak preferred long axis orientations (V_1 axes) spread out in a way that is incompatible with what would be expected in a subglacial environment characterized by sediment deformation (e.g. Benn and Evans, 1996; Larsen and Piotrowski, 2003).

6. The Kipholstjärnen section

At Kipholstjärnen, situated ca 500 m northwest of the Eggling site, three Rogen moraine ridges, 10–15 m high,

lie in close proximity (Fig. 4). An old section, opened up for road-building in 1964, occurs in the horn-shaped end of one of these ridges. It was briefly documented by Nordell (1984) and also by Lundqvist (1997). The exposure, from which considerable volumes of sediment have been removed, has a wall centred below and more or less paralleling the crest-line of the horn. The section was cleared and then gradually deepened by an excavator in three steps, finally covering a total height of ca 11 m and a width of ca 20 m.

6.1. Sediment description

The intricate sedimentary structures of the Kipholstjärnen section (Fig. 9) are readily discerned due to colour differences between diamict units; a reddish diamicton, an olive-green diamicton and a dark grey diamicton. The ridge surface is covered by abundant large boulders, dominated by Digerberg conglomerate. These, however, are totally absent in the diamict sediments forming the ridge.

6.1.1. Reddish diamicton

This is a matrix-supported, gravelly-sandy diamicton (gravel 20–35%; sand 40–55%; silt 15–20%), the colour coming from a very high content of porphyries. The gravel contains 21–38% of Bredvad porphyry (Fig. 6) and 21–31% phenocryst-rich porphyry, with a mean total porphyry content of about 38%. The reddish diamicton is the dominant diamict facies, intercalated with the olive-green diamicton in the northern part and with the dark grey diamicton in the southern part of the section.

The reddish diamicton starts at the base of the section as a vaguely stratified deposit, partly due to a diffuse subhorizontal lamination within the diamicton itself, enhanced by thin, intermittent gravel stringers, and partly due to the frequent occurrence of 0.5–1.5 cm beds of fine sand. In places, these sand beds are thicker and show an internal planar-parallel lamination. The stratified part of the diamicton grades upwards without any clear boundary into a massive diamicton and is intercalated with or occurs as pods within the other two diamict facies. The matrix-supported parts of the reddish diamicton are replaced locally by a clast-supported deposit, sometimes occurring as more diffuse, lens-shaped bodies and sometimes occurring as stretched-out, inclined and/or undulating clast-rich bands.

Two fabric analyses were carried out in the lowermost stratified part. The fabric plots (Fig. 10) reveal unimodal and clustered (Fig. 8) fabric shapes with strong to very strong preferred clast long-axis orientations (S_1 eigenvalues = 0.769 and 0.821). The V_1-axis orientations (azimuths 343° and 326°) are approximately perpendicular to slightly oblique to the general trend of the ridge crest, but oblique to the horn orientation.

6.1.2. Olive-green diamicton

This is a hard, massive, matrix-supported, sandy-gravelly diamicton (sand 25–35%; gravel 45–60%) with a silt content of 10–20%. The diamicton is olive-green when fresh but yellowish when dry. This colour is due to 79–99% of Öje diabase (mean content 92%; Fig. 6) in the gravel. The diamicton forms beds that range from 10 cm up to 1.5 m in thickness. These beds are not planar in their geometry but usually diverge/converge in an undulating pattern or meet at both ends, interbedded with or enclosing the reddish diamicton, and are in fact large overturned folds, probably representing sheath folds (see below). At places the olive-green diamicton can also be found as detached, more or less stretched-out clasts within the reddish diamicton.

6.1.3. Dark grey diamicton

This is a very compact, massive to weakly stratified, matrix-supported to near clast-supported, gravelly diamicton (fine to medium gravel 60–70% of sediment <20 mm). The content of coarse gravel and small cobble clasts is at places very high and the clasts usually have sharp edges. The diamicton has a higher content of boulders than the other diamict facies and also carries some very large (up to 2 m in diameter) boulders. The colour, very dark grey to nearly black when fresh and greyish when dry, is related to the dominance of one lithology; analysed gravel samples show 80–98% of black rhyolite, rich in small vesicles (Fig. 6). This rhyolite also dominates the boulder-sized clasts.

The dark grey diamicton is weakly stratified in its lower part with thin (0.5–1 cm) beds of coarse sand, gravel stringers and clast-rich horizons, all lying subhorizontally. However, in the basal part, especially between marks 11 and 14 m (Fig. 9), these beds rise gradually into a vertical position and are eventually overturned beneath a shear surface. Sorted sediments occur as isolated and imbricated clasts within the diamicton or as interfingers from the reddish diamicton.

6.1.4. Structural geology

From the bed contacts in the section wall it is obvious that all sediment above ca +2–3 m (Fig. 9) have experienced a ductile non-penetrative deformation, resulting in large-scale folding of the primary sedimentary units. A number of measurements on tectonic structures such as shear planes, fold limbs and overturned clast horizons (Fig. 11) indicate a stress direction from NNW ($S_1 = 0.935$). This is perpendicular to the main trend of the ridge but oblique (ca 50°) to the crest-line of the horn. The lower boundary of the deformed sediment sequence is by no means clear. The boundary is a gradual one with a change from vaguely stratified

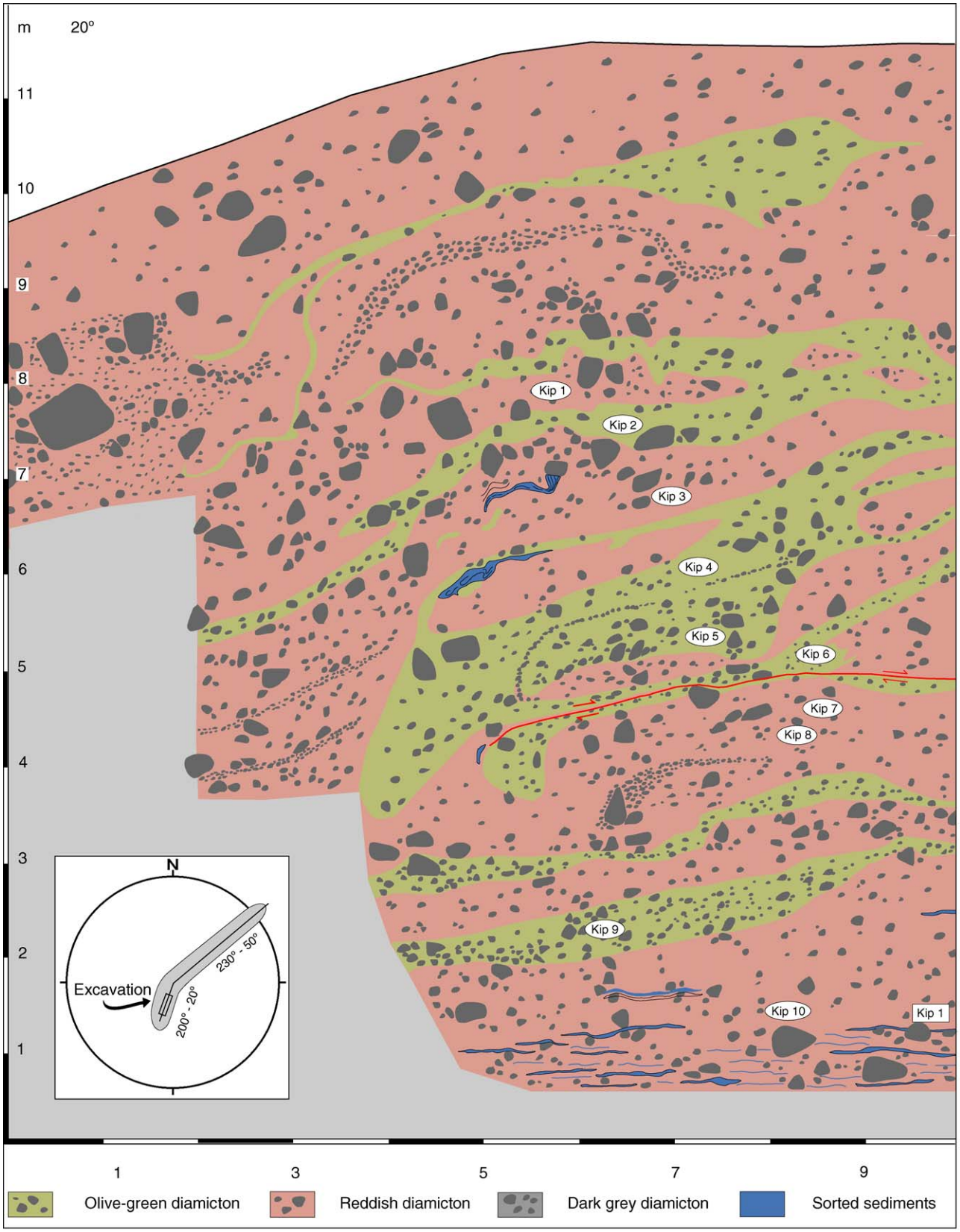

(A)

Fig. 9. Section through the Kipholstjärnen moraine. The section is near-parallel to the crest-line of the horn, which is at an angle of ca 30° to the main trend of the ridge. The section wall was documented at a scale of 1:25, here presented in full at a scale of ca 1:60.

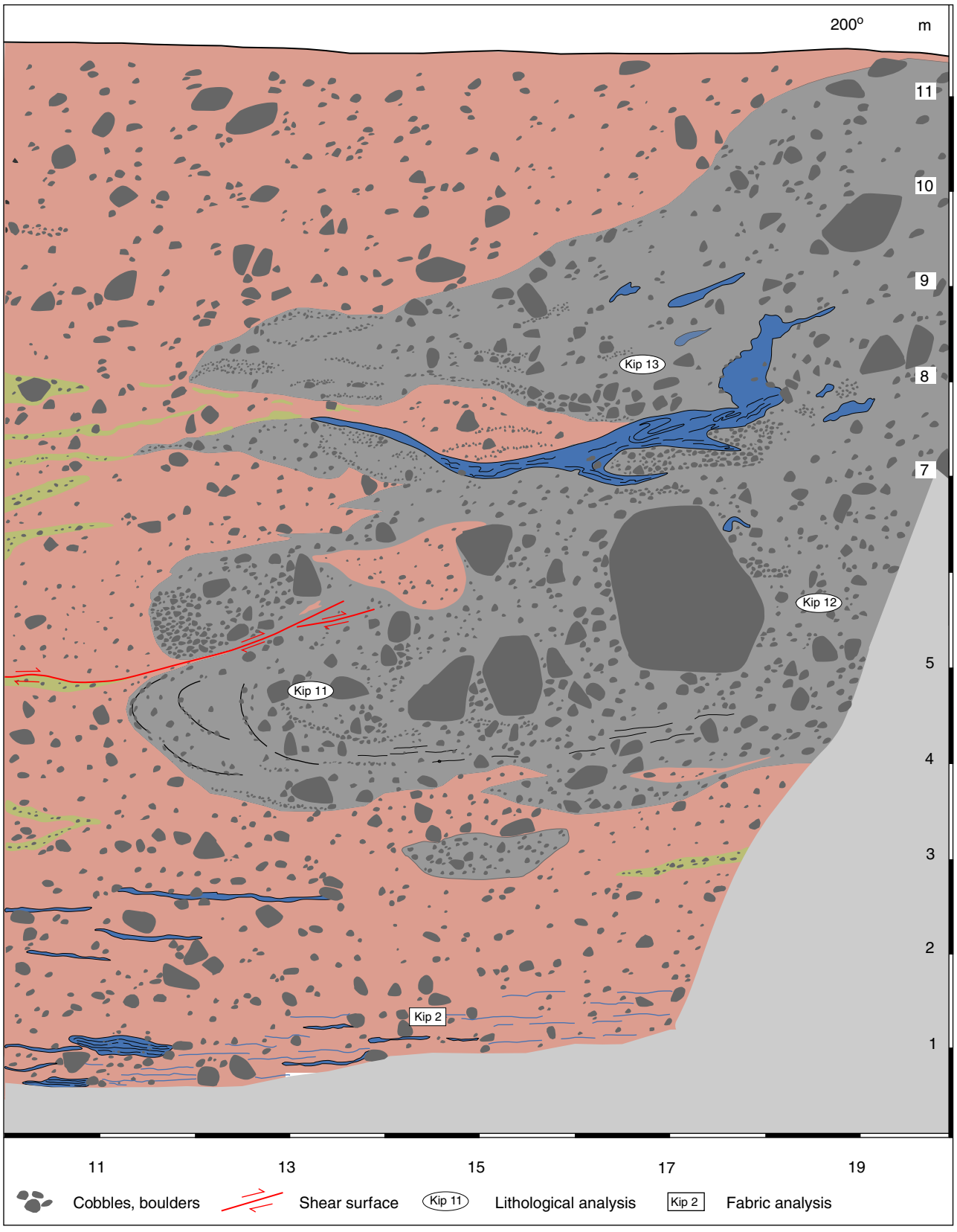

(B)

Fig. 9. (*Continued*)

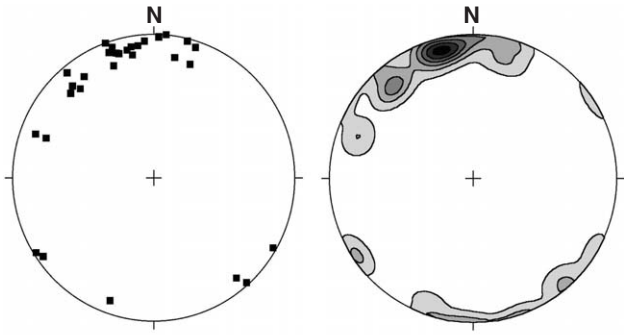

Kipholstjärnen 1			
n = 30	V_1 = 343°/8°	V_2 = 252°/6°	V_3 = 130°/80°
	S_1 = 0.769	S_2 = 0.213	S_3 = 0.018

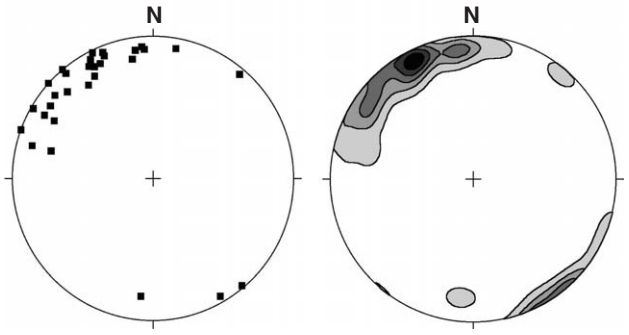

Kipholstjärnen 2			
n = 30	V_1 = 326°/9°	V_2 = 235°/5°	V_3 = 117°/80°
	S_1 = 0.821	S_2 = 0.158	S_3 = 0.021

Fig. 10. Schmidt equal-area, lower-hemisphere projections of clast long-axis orientations from the Kipholstjärnen section (Kip 1, Kip 2; for location, see Fig. 9). Both scatter plots and contoured diagrams are included for each fabric as well as calculated eigenvectors (V_1, V_2, V_3) and normalized eigenvalues (S_1, S_2, S_3) according to Mark (1973).

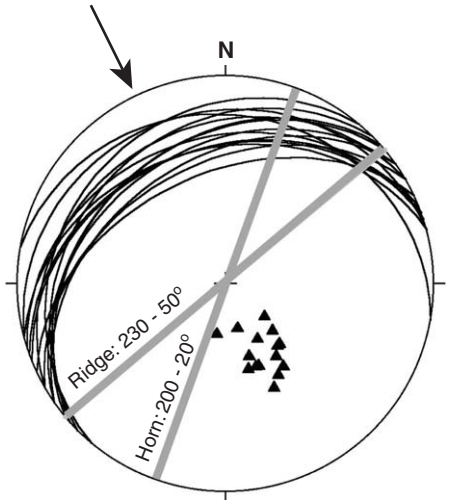

Kipholstjärnen, tectonic structures			
n = 15	V_1 = 332°/32°	V_2 = 241°/2°	V_3 = 147°/57°
	S_1 = 0.935	S_2 = 0.050	S_3 = 0.016

Fig. 11. Schmidt equal-area, lower-hemisphere projections of tectonic structures from the Kipholstjärnen section. The measured tectonic structures include strike and dip of shear planes and fold limbs, plotted as great circle planes and poles to planes. The interpreted stress direction (arrow) is from NNW (V_1 axis), which is approximately perpendicular to the ridge crest line.

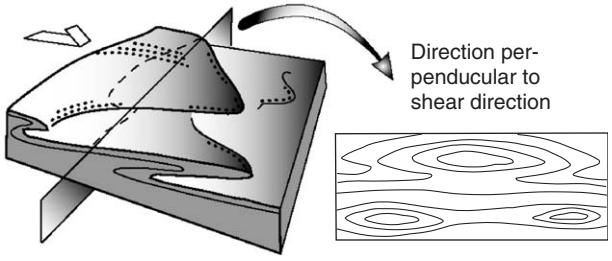

Fig. 12. Cartoon (redrawn from van der Wateren et al., 2000) showing the three-dimensional structures of sheath folds. The folds appear as low-angle attenuated isoclinal folds parallel to deformation direction, whereas they form eye or concentric ring shapes in a section perpendicular to the shear direction (van der Wateren, 1995; van der Wateren et al., 2000).

diamicton, interbedded with subhorizontally bedded sorted sediments with preserved internal lamination, into the over-lying deformed sequence of diamict and sorted sediment beds (ca 1–2 m above the base of the section).

It was observed that lens/pod-shaped bodies of reddish or olive-green diamicton gradually grew smaller or larger both laterally along the section wall and, with excavation, into the section wall, i.e. a 3D expansion/reduction of the sedimentary bodies. The development of such structures can be demonstrated from a tectonic model with three-dimensional cylindrical folding (Fig. 12), resembling overturned sheath folds (van der Wateren et al., 2000). When cut parallel to the dominant shear direction these folds appear to indicate a linear fold axis perpendicular to the stress direction. However, perpendicular to the stress direction (Fig. 12), sedimentary boundaries turn up as lens-shaped, indicating three-dimensional fold noses drawn out in the bulk shear direction (van der Wateren et al., 2000). In exposures oblique to the main stress direction, as is the case in the Kipholstjärnen section that parallels horn-crest direction (Fig. 11), these fold noses are projected in the section wall as more or less drawn-out deformational structures, differing from perfect lens-shaped sediment bodies, as shown in Fig. 12.

Some of the sorted sediments intercalated with the diamict facies (e.g. the sediment bed above the large boulder at 17 m/+6 m, Fig. 9) show isoclinal folding with attenuated fold limbs of internal primary

lamination and also some well-developed rootless intrafolial folds. These indicate the development of ductile shear zones. The detached, folded bodies are made up of coarser material, lying in more fine-grained sediments as a result of differences in sediment rheology under applied shear stresses at deformation.

At least one brittle-deformation shear zone, ca 9 m long in the projection of the section wall, was identified (Fig. 9, between marks 5–14, ca 5 m above base of the section). Starting at the 5 m mark, reddish diamicton is sheared into a shear zone cutting olive-green diamicton. Further to the right (from 8.8 m mark) the bed boundary between reddish and olive-green diamicton seems to have localized the shear surface, which forms a 1–3 cm thick shear band consisting of crushed, extremely angular porphyry in coarse sand-fine gravel grades. This shear band continues into the dark grey diamicton (at 11.8 m mark) and, after splitting into two, disappears. As mentioned above, there is a gradual increase in clast horizon and individual clast imbrication of the dark-grey diamicton, with a total overturning of clast horizons just beneath the described shear zone. This indicates a shear-stress transfer, resulting in ductile bending/folding beneath, and contemporaneous with, the brittle-deformation shear band. In this specific case the brittle-shear zone cuts through the folded olive-green/reddish diamicton and thus post-dates the ductile deformation phase producing the sheath folds. On a general scale it is likely that both ductile and brittle deformation occurred at the same time during the whole deformational event.

6.2. Sediment and process interpretations

The lowermost part of the section cuts down into sediments beneath the morphological expression of the ridge; thus the Kipholstjärnen section represents a full sediment sequence of the horn-shaped part of a Rogen ridge. On the basis of the sediment properties and fabric of the reddish, weakly stratified diamicton at the base of the section, the most plausible interpretation is that this diamicton is a basal till. However, conclusive evidence of which type of basal till is not at hand. The small-scale intra- and interlamination within the diamicton could be taken as evidence of subglacial shear banding in a deforming bed zone (Benn and Evans, 1996), an interpretation which also could be supported by the fabric data. However, diagnostic criteria for a deformation till interpretation are missing (e.g., small-scale folding and boudinage structures). An equally appropriate interpretation would be basal melt-out till with an inherited englacial stratification and fabric preserved during the melt-out processes, the stratification enhanced due to winnowing-out and deposition of sorted sediment beds along the melting glacier/bed interface (Shaw, 1982, 1983; Möller, 1987). Additionally, the very high strength of the fabric data supports such an interpretation (e.g. Dowdeswell and Sharp, 1986).

The primary genesis of the diamictons making up the ridge in the Kipholstjärnen section is difficult to deduce from any of the sedimentary properties. Due to the post-depositional deformation the original bed configurations are obscured, and the sequence is repetitive due to thrusting and folding. In spite of this, distinct lithological differences between the three observed diamict facies are preserved and must represent some sort of primary release of debris from a glacier that here, as opposed to the Eggling site, was distinctly stratified with regards to debris lithologies, probably as a result of little vertical mixing during transport of the debris after incorporation into the glacier or, alternatively, into a deforming layer.

There are three possible explanations for the (primary) origin of the diamict beds above the stratified diamicton at the Kipholstjärnen site. One plausible explanation to the distinct lithological banding is in situ basal and/or supraglacial melt-out of englacial debris bands, possibly from transversely arranged, stacked sequences of debris-rich ice, as proposed by Shaw (1979) in his original model for Rogen moraine formation, or as proposed in the model of 'Åsnen moraine' formation in southern Sweden (Björck and Möller, 1987; Möller, 1987). This would not just form a sediment source, but also precursor ridges for later deformation into Rogen shapes.

However, the preservation potential of thick melt-out till sequences has been debated (Paul and Eyles, 1990; Menzies and Shilts, 1996). If, as an alternative to melt-out till deposition, we infer the same depositional environment as indicated from the stacked sequence of debris-flow deposits at the Eggling site, this would mean that glacial debris after melt-out was redistributed by mass-flow processes directly into the final position of deposition, most probably into troughs between adjacent ice-cored moraines. This model infers a direct sediment transfer, or else any distinct lithology differences inherited from the stagnant ice would be obliterated due to sediment mixing during a series of successive back/down-wasting and debris-flow events until the final deposition took place. A possible parallel to such a lithological stratification is reported by Benn (1992) from hummocky moraines in Scotland, interpreted as formed by stacked/interbedded debris flow and glaciofluvial deposits in an ice-contact environment.

A third model is stacking of deforming bed sediments due to "constructional glaciotectonic deformation" (Hart and Boulton, 1991), i.e. gradual 'freezing' of deforming bed sediments over a particular area, producing a positive landform. If the deforming bed carries specific lithologies over specific periods of time, then it would theoretically be possible to recognize these in the stratigraphic record.

However, as the Kipholstjärnen site clearly demonstrates that the primary genesis of the sediment enclosed in the horn-shaped part of the Rogen ridge has very little to do with the present configuration and position of the sediment, but much more with a post-depositional deformation history, it can then be concluded that final landform build-up is not coupled to primary sediment deposition at this site. The observed folds and thrusts in the ridge indicate a horizontal shortening of the strata due to shear-induced compressional strain in the subglacial bed, combined with a stress-parallel translocation/extension of the ridge sediments, as indicated by the bent planform of the ridge end. The coexistence of both ductile and brittle style deformation structures within the succession further demonstrates the complexity in sediment rheology and deformation kinematics.

7. A model of Rogen moraine formation

The geomorphic constituents of a classical Rogen moraine are ice flow transverse elements, the main ridge, and the more or less prominently developed longitudinal elements, the horns, pointing in a down-ice direction. Based on sedimentological, structural and geomorphological data from the two sites it appears that the sediment in the mid-ridge position at the Eggling site was not deposited by any subglacial deformational processes. Furthermore, no observable structures indicate that the primary geomorphology (i.e. the transverse element, the ridge) is due to glaciotectonic deformation and/or stacking. On the other hand, the Kipholstjärnen site clearly demonstrates that the sediments forming the longitudinal, horn-formed element of the Rogen moraine have experienced a deformational event to such a degree that it is impossible to decode the original genesis of the sediments included in the deformation. Based on the sedimentological and structural data from this investigation it is also suggested that not only sediment build-up predates the final landform-shaping event, but also the sediments were spatially arranged in precursor ridges or linearly arranged hummocks prior to remoulding into a Rogen moraine landscape. This scenario, and the palaeoenvironmental and chronological implications that follow from this are now further elucidated.

7.1. Sediment build-up and precursor ridge formation

I propose that the main bulk of sediments enclosed within the present Rogen moraine ridges were deposited prior to the final shaping into Rogen ridges, the latter more or less defined by the formation of horns. The bulk of the sedimentological criteria at Eggling suggests that the sediments were stacked in a sequence of sediment gravity flows. Further, the absence of tectonic thrust structures indicates that the sediments are in their original position of deposition. Several models for the precursor ridges are plausible. The spatial pattern of the moraine ridges in the Indån valley, with ridge main-axis orientations transverse to valley axis and a topography-controlled ice-flow direction, suggest a glacially active control during the formation of the precursor ridges. This could be similar to the production of the linear Scottish 'hummocky moraines', which according to Benn (1992) and Bennett and Boulton (1993), resulted from sediment gravity-flow and glacier pushing at the margins of actively retreating ice lobes.

Another possible model is one that produces ice-flow-transverse supraglacial debris concentrations close to the glacier margin. This could be by means of folding and thrusting of debris-rich ice, leading to differential ablation on the glacier surface and eventually to the formation of a marginal system of ice-cored moraines (Fig. 13). This is similar to what was described by Boulton (1972) for the active margin of the Elisebreen glacier on Spitsbergen and to what Paul (1983) described as marginal 'ridge-trough' systems. Sediments released by melt-out will be redistributed during down- and back-wasting (cf. Eyles, 1979, 1983; Paul and Eyles, 1990; Krüger and Kjær, 1999; Kjær and Krüger, 2001) and transported by means of different gravitational processes (e.g. flow, spall, slump; cf. Lawson, 1988) into the troughs between the stagnant ice ridges. There, depending on the presence and energy level of fluvial processes, the sediment gravity flows would be more or less integrated, reworked or disaggregated into the fluvial system and its sediments. The sedimentary succession, its properties and architecture, as demonstrated from the Eggling section, parallels what Paul (1983) defined as a typical sequence of a trough receiving mainly sediment gravity flows. From this it should also be expected that the succession continues downwards into a basal melt-out till. This is, however, not demonstrated from the Eggling section, although the base of the sequence was not exposed (see, however, the basal part of the Kipholstjärnen section). The final landform-generating process in this depositional environment should be one of landscape inversion (Boulton, 1972). During this process, ice-cored moraines would finally melt down forming depressions and the former low-lying sediment-receiving trough areas would eventually form topographic highs as ridges and controlled hummocky moraine (Fig. 13).

7.2. Deformation of the ridges

As demonstrated by planforms of Rogen ridges in the Indån area, reshaping of the precursor ridges into Rogen shape varies from very little (slight bending of just one ridge end for ridges lying in a valley-lateral position) to 'boomerang' reshaping, usually of those

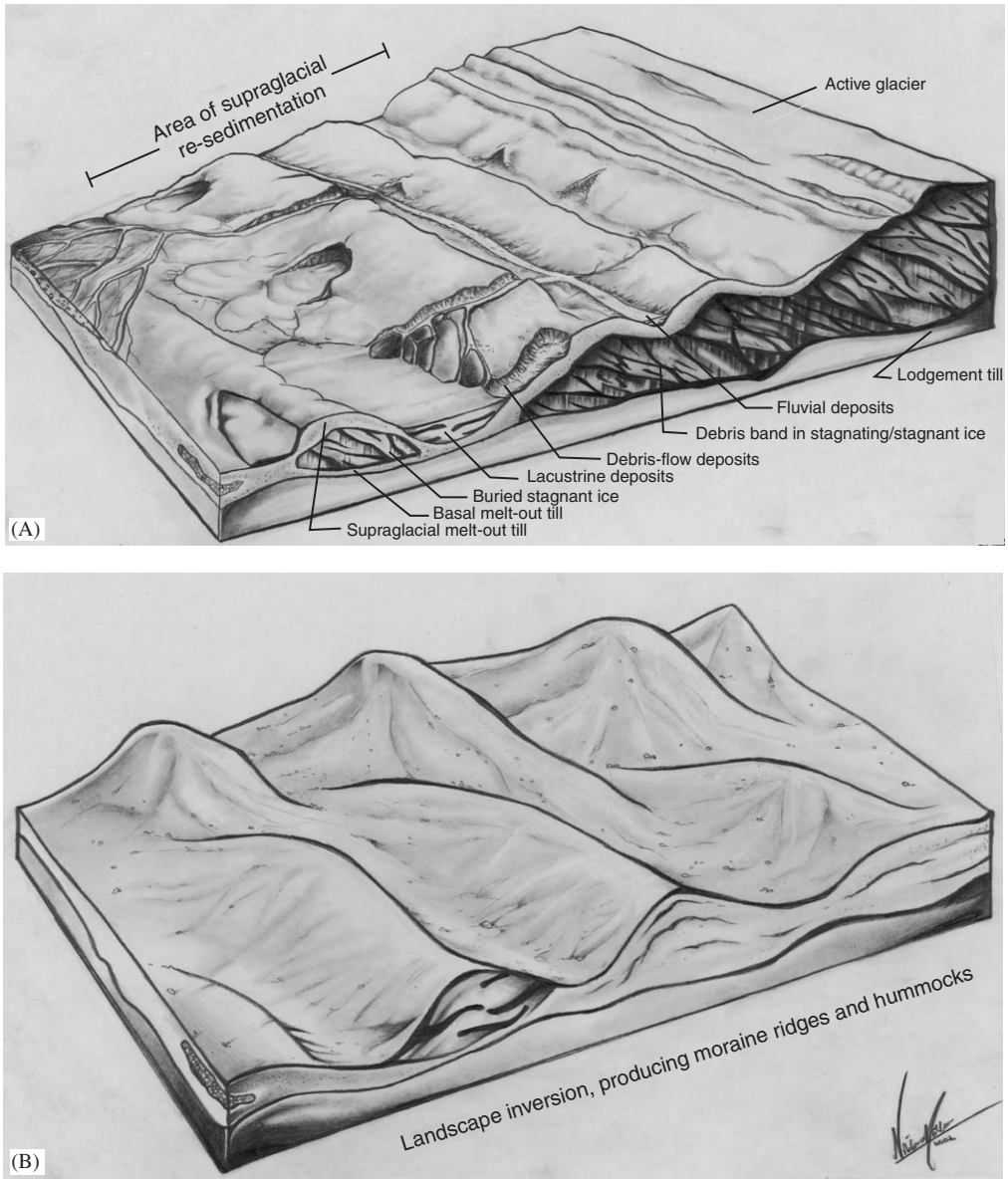

Fig. 13. A model of controlled moraine formation. Panel (A) redrawn from Edwards (1986); whole concept primarily from Boulton (1972). (A) A zone of ice-cored moraines develops in front of an active glacier during slow retreat. Debris is melted out on the glacier surface which, due to back- and down-wasting, is re-distributed by means of gravitational processes into the moraine-parallel troughs as debris-flow deposits. Depending on fluvial activity these sediments can be disaggregated and transformed into glaciofluvial sediments. Ponded water within troughs can give rise to lacustrine deposits. (B) During final melt-out of stagnant ice a landscape inversion takes place with the variable trough sediments forming ridges and hummocks, and previous locations of ice-cored moraines forming low-lying areas, now occupied by lakes and bogs.

ridges lying very central in the valley (Figs. 3 and 4), but never a complete transformation into ice-flow-parallel ridges. These differences in reshaping are schematically demonstrated in Fig. 14, with reshaping stages II–V present in the Indån valley, but not developing further into the hypothetical reshaping stages VI–VII (parabolic to elliptic drumlin shapes). The observed sheath folds and shear bands with crushed porphyries in the Kipholstjärnen section indicate high strain at deformation; sheath folds usually form at strain rates of $10\,a^{-1}$ or more (Cobbold and Quinquis, 1980; van der Wateren, 1995). Given sufficient time with such high strain rates, compressional shortening of sediments would be combined with horizontal flattening and extension, gradually transforming a transverse element into longitudinal landforms (cf. Boulton, 1987; Clark, 1994). The varying but limited reshaping, always starting in the lateral end(s) of the precursor ridges thus tell us that the finite time for deformation must have been short at the indicated high strain rates and that deformation could not have been uniform over the bed but instead localized, probably in response to the

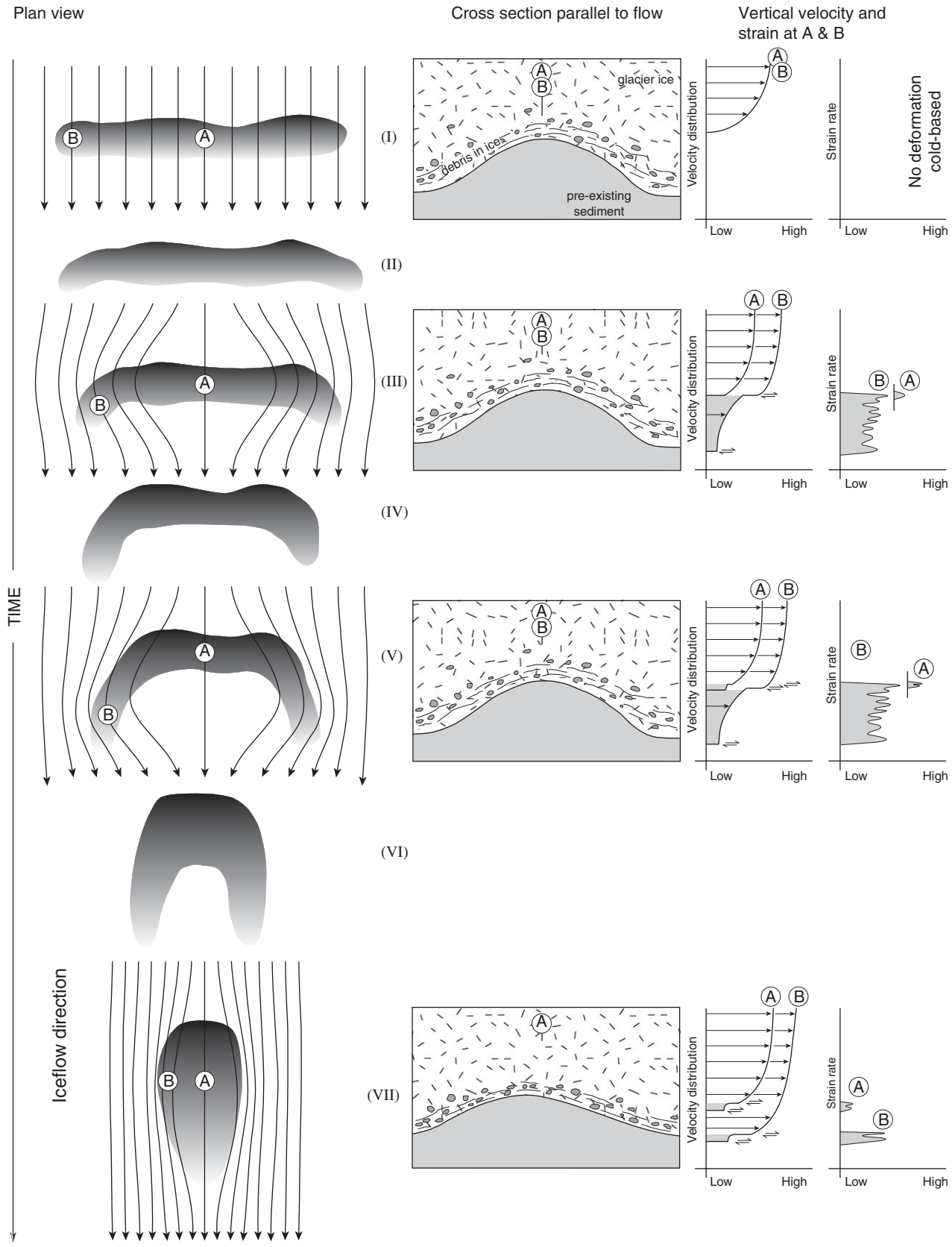

Fig. 14. Proposed reshaping stages of an initially linear transverse precursor moraine (I) into successively more curved and elongated Rogen moraine ridges (II–V), hypothetically ending up with the formation of parabolic (VI) or elliptic drumlins (VII). Rogen moraine shapes II–V are present in the Indån valley, but forms resembling stages VI–VII have not been identified there. Flow lines around the obstacle to flow and principal velocity-distribution and strain-rate differences between mid-ridge and ridge-end positions are indicated.

existing bed morphology. Short deformational events can occur far inside an ice margin if there is a mosaic of deforming/non-deforming spots changing in time, as proposed by Piotrowski and Kraus (1997) and Piotrowski et al. (2004). However, a short deformational event can also be the case if basal conditions for this are at hand only in the near-marginal area and terminated due to deglaciation. Near-marginal deformation is supported by the planforms of the Rogen ridges, lying transverse to the gradually changing valley-axis direction and thus indicating a topographically controlled ice flow. The very clear difference in reshaping, as indicated from the difference in curvature of ridge axes, between the lateral and central parts of the Indån valley must thus either have been a response to a somewhat longer period of deformation and/or somewhat higher strain rates in the central parts, compared to the lateral parts of the valley.

Ice-marginal deformation is likely also due to the gradual build-up of glaciotectonic stresses towards a glacier margin, combined with a reduction of shear strength due to increasing porewater pressure as the subglacial bed goes from frozen to melted (see below). The latter circumstance, with a basal regime going from interior cold-based conditions to wet-based conditions at the margin of the retreating Late Weichselian ice sheet over northern Scandinavia has been convincingly demonstrated by the research group of J. Kleman (Kleman, 1992, 1994; Hättestrand, 1997a; Kleman and Hättestrand, 1999; Kleman et al., 1999; see Fig. 1A), a model deduced from the preservation of older glacial landforms originally suggested by Lagerbäck (1988a, b). This is also the prerequisite for the 'fracturing model' for ribbed moraine formation (Hättestrand, 1997a; see Fig. 15).

The suggested reshaping phase cannot be deduced from any deformational structures in mid-ridge position, as demonstrated from the Eggling site. However, the subhorizontal bedding of primary precursor-ridge sediment, cut by the sloping proximal ridge slope (Fig. 5b) might indicate that this is an up-glacier erosional surface and that slumped debris-flow units, still present on the distal side of the ridge were evacuated during the reshaping event.

The Digerberg conglomerate boulders, covering the surface of Rogen moraines along the eastern Indån valley side most likely belong to the re-shaping phase. According to the bedrock geology map (Hjelmqvist, 1966) Digerberg sedimentary rocks form the local bedrock in most parts of the valley, but the thick overlying Quaternary sediments appear to be devoid of them. The source area is thus not a local one but most probably an area with Digerberg conglomerate in an up-flow direction and with a thin coverage of Quaternary sediments. The obvious choice for this would be the Hykjeberg area 15 km towards the NW (Fig. 1), which is a bedrock plateau at more than 500 m a.s.l. The surficial distribution of these boulders thus suggests that they were quarried, incorporated and transported englacially in Late Weichselian ice that, after the re-shaping of precursor landforms, did not lodge the conglomerate boulders but rather draped them as a boulder train on the emerging subglacial surface during deglaciation.

7.3. *Summary of the Rogen moraine formation model and its palaeoenvironmental and chronological implications*

The field results agree with a two-step model of Rogen moraine formation, originally suggested by Lundqvist (1989, 1997). Sedimentary facies and architecture in mid-ridge position suggest precursor moraine formation as a result of sediment gravity-flow infill of inter-ridge troughs. These troughs were paralleling a system of ice-cored moraines, developed transverse to ice flow in the valley-based part of the receding ice sheet, forming a frontal, stagnant part of the glacier and eventually leading to a process of landscape inversion. Contrary to this, the sedimentary facies and architecture in lateral horn positions suggest active deformational processes of pre-existing sediments by means of folding and thrusting at high strains, reshaping ridge ends in a down-flow direction. The draping boulder blanket with a lithology not present within the ridge sediments, suggests that this is related to a passive release from the glacier after the deformational stage. We thus have a scenario of stagnant ice deposition followed by active ice deformation and reshaping. If these events took place during the same glacial cycle they record local deglaciation followed by a major glacier re-advance. The latter is not supported from what we know of the Preboreal deglaciation history for areas in a central position of the last Scandinavian ice sheet; instead the deglaciation history implies a frozen-bed ice sheet which, at a very late stage, became wet-based and melted fast due to an extremely negative mass balance in the early Holocene (e.g. Kleman, 1994; Kleman et al., 1997). My depositional model for precursor moraine formation fits much better with a marginal area of a west-centred, presumably Early Weichselian, Scandinavian ice sheet (Kleman et al., 1997), receding at a much slower pace in an interstadial sub-polar environment. This scenario is linked to the paradigm shift within glacial geology that took place in Scandinavia during the 1980s. Previously, the glacial landscape was regarded something as more or less totally created during the latest glaciation. However, it became obvious that large parts of Scandinavia retains a glacial geomorphology that was created during Early Weichselian glaciations, which with only minor modifications survived the latest glacial event (the Late Weichselian glaciation). This was convincingly demonstrated by Lagerbäck's work on eskers, drumlins and Veiki moraines in central parts of Norrbotten, northern Sweden (Lagerbäck, 1988a, b;

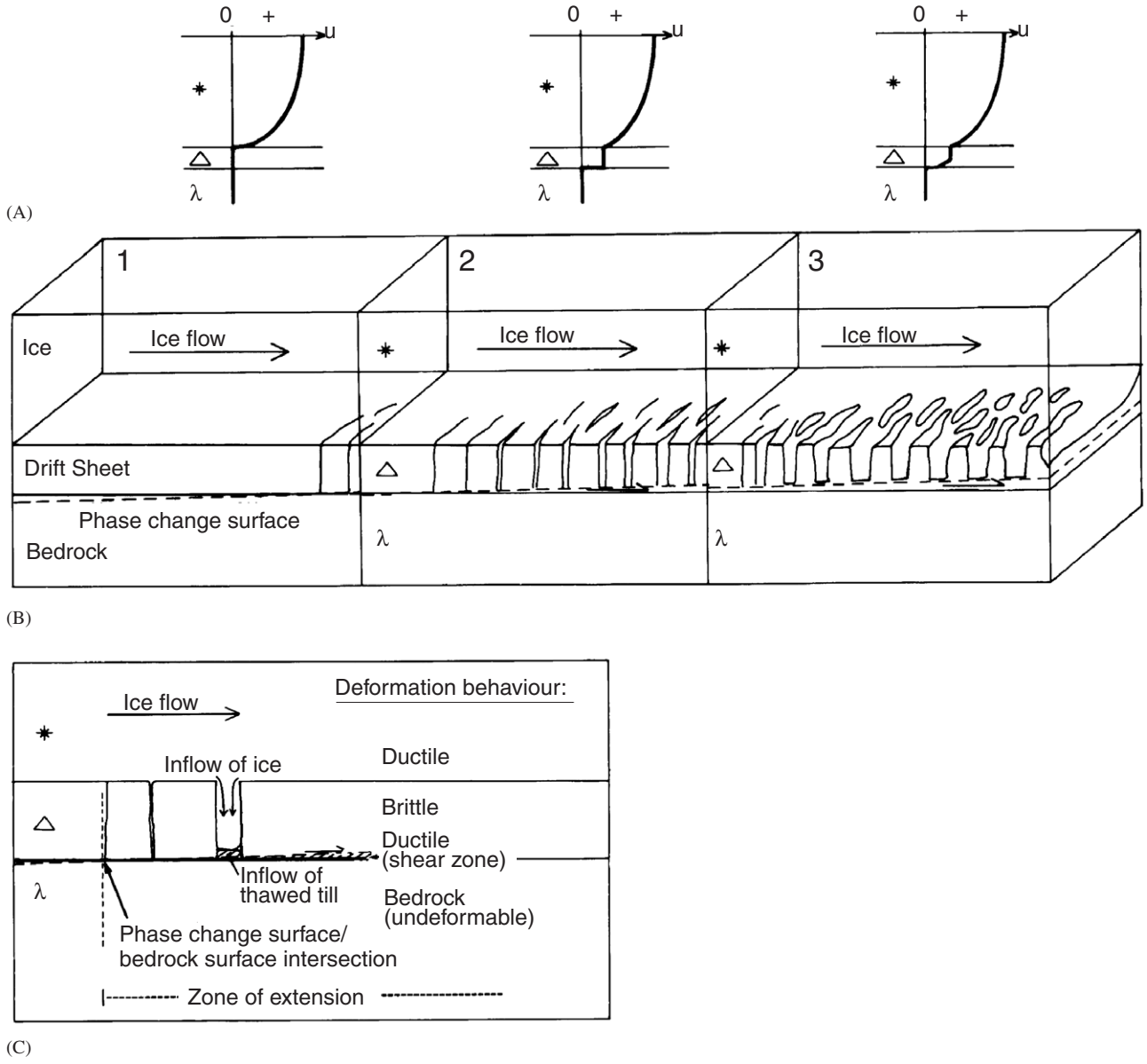

Fig. 15. Model of ribbed moraine formation according to Hättestrand (1997a), implying the fracturing of a pre-existing drift sheet during the transformation from cold-based to, in distal direction, warm-based conditions under a deglaciating ice sheet. (A) Ice flow velocity (u) profiles in the lower part of the ice mass for stages 1–3 in b. (B) Time slice boxes (1–3), showing the successive evolution from a pre-existing drift sheet to a ribbed moraine pattern. Detachment of frozen drift ribs starts to occur when the pressure-melting isotherm (Phase Change Surface; PCS) intersects the bedrock surface. (C) Close-up of the fracturing zone. (Reprinted from Sedimentary Geology, 111, Hättestrand (1997a), with permission of Elsevier Science).

Lagerbäck and Robertsson, 1988). It was later established by the research group of J. Kleman (Kleman, 1990, 1992, 1994; Kleman and Borgström, 1990, 1996; Kleman et al., 1992, 1997; Hättestrand, 1994; Borgström, 1999) that relict or palimpsest landscapes are not just restricted to the northern parts of Sweden, but frequently occur southwards—both as patches or as wider areas—along the Scandinavian mountain range and foothill areas down to at least the province of Dalarna (ca 61 °N) due to preservation beneath a Mid- to Late Weichselian cold-based ice sheet.

8. Discussion

8.1. Comparison to other models of Rogen moraine formation

The field evidence from Rogen moraine in the Indån area appears to support the two-step model of Rogen moraine formation originally proposed by Lundqvist (1989, 1997). The genetic model proposed above also supports the views held by Boulton (1987) and Clark (1994) that various kinds of pre-existing linear

landforms, lying transverse to ice flow, can be transformed into new ones that parallel the new flow direction. If reshaping stops prior to total remoulding into new longitudinal landforms, then the preserved result would be Rogen moraines.

However, can the sedimentological and structural features encountered in the Eggling and Kipholstjärnen section be supportive of other more recent models of Rogen moraine formation? The Shaw (1979) model of Rogen moraine formation (c.f. Aario, 1987; Bouchard, 1989) suggest that the features begin as debris-rich ice that, after stagnation, melts out in situ, forming Rogen moraine entirely consisting of melt-out till. This implies that fold structures, such as those shown at the Kipholstjärnen site, represent englacial folding of debris-rich ice that is later preserved. However, the shear planes, lined with crushed porphyry clasts and cutting the fold structure would hardly form—and be preserved as they are seen today—if this process occurred within debris-rich ice. Furthermore, an alternative interpretation as a melt-out till sequence for the sediment succession at the Eggling site is not justifiable from observed sedimentary structures and properties. It is thus concluded that the Shaw (1979) and other similar melt-out models for Rogen moraine formation are not applicable as an alternative to the proposed two-step model. Even if melt-out of debris-rich folded ice sequences did act as a depositional ridge, other processes, such as stacked flow-till accretion, could equally well provide precursor ridges for later reshaping into Rogen moraines.

Much cited recently is a 'one-step' model for ribbed (Rogen) moraine formation, first introduced by Hättestrand (1997a) and later discussed by Hättestrand and Kleman (1999) and Kleman and Hättestrand (1999). This model proposes fracturing and extension of a subglacial frozen drift sheet, the fracturing arranged in transversely oriented sediment blocks that were passively dragged along by the glacier above a décollement plane, situated at the boundary between bedrock and the overlying drift sheet (Fig. 15). The displaced blocks of the fractured drift sheet (the precursor moraines in this model) form the ribbed moraines, and the inter-ridge troughs represent areas of extension. One of the main arguments supporting this model is that "…the shape of individual ribbed moraine ridges match each other, like a jig-saw puzzle" which "…cannot be explained by shearing and stacking" (Kleman and Hättestrand, 1999, p. 58). Hättestrand (1997a) is also of the opinion that ribbed moraines are not formed in an ice-marginal environment due to the facts that they are often drumlinized and overrun by eskers, and an approximate minimum distance in orders of tens of kilometres behind the ice margin is suggested. A prerequisite for the model is that the ice sheet at deglaciation had an outer melted bed zone and an inner frozen bed zone. A consequence of this is that the distribution of ribbed moraines should be exclusively linked to areas having these basal-regime conditions at deglaciation. Hättestrand and Kleman (1999, Fig. 7) show that there is a good match between the distribution of ribbed moraines in Scandinavia and areas with frozen-bed conditions during the Late Weichselian (LGM; Fig. 1A).

The two models, the 'glacial reshaping model' proposed in this paper and the 'fracturing model', have one important similarity; they both require a glacial–deglacial basal thermal regime pattern with an inner frozen-bed zone and an outer melted-bed zone. In spite of this there is a fundamental difference between the two models. The 'reshaping model' puts the primary landform formation in an earlier deglacial event, followed by a reshaping during a succeeding glacial–deglacial; the frozen-bed zone is needed to preserve precursor landforms prior to the deformational phase. The 'fracturing model' postulates a ridge formation due to extensional fracturing of a pre-existing drift sheet followed by deformational reshaping during the same deglacial event. Hättestrand and Kleman (1999) gave a comprehensive review of ribbed moraine characteristics, summarized in fourteen notes that "any theory of ribbed moraine formation must be compatible with, and be able to explain" (op. cit., p. 56). The 'reshaping model' is compatible with, and can explain all these demands except one (no. 11): "often display a 'jig-saw puzzle matching' of the ridges". However, this demand contains a measure of subjective interpretation, and there are many areas where this puzzle matching is difficult to see. The field data from the Indån valley do not give any conclusive evidence against the 'fracturing model' other than that the ridges appear to be in place, that is, the sediment at the Eggling site lacks any evidence of deformation from a supposed tensional phase, and the sediment at the Kipholtjärnen site shows continuous diamicton from below the ridge up into the ridge.

8.2. *The 'fracturing model'—a critical discussion*

The main problem with the 'fracturing model' (Hättestrand, 1997a), apart from a lack of supporting sedimentological and structural field evidence, is theoretical; the model can be strongly questioned along two independent lines of argument, one based on soil mechanics and the other on the geomorphologic consequences of the model.

8.2.1. *The soil mechanics counter-evidence*

The 'fracturing model' (Fig. 15) states that when the PCS (the zero degree isotherm) "reaches the bedrock–drift boundary, or immediately above, deformation may take place at the bedrock–drift interface, or within

the lower thawed part of the drift sheet, where the shear strength is low'' (Hättestrand, 1997a, p. 52). However, it is not self-evident that the shear strength is lower when the drift sheet is thawed, nor is it self-evident that the induced glaciotectonic stress would be higher than the shear strength. The crucial parameter would be pore-water pressure and its inter-relation to shear strength.

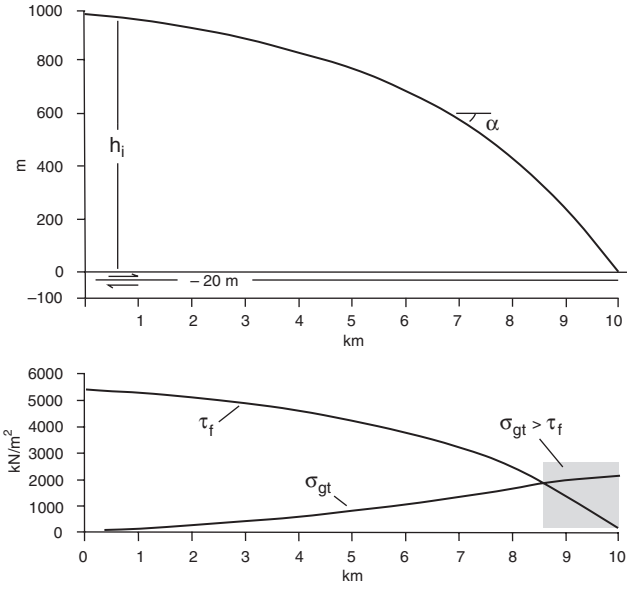

Fig. 16. Upper panel showing a typical profile for the outer part of an ice sheet (redrawn from Aber et al., 1989), and lower panel a plot of calculated total glaciotectonic stress (σ_{gt}) and shear strength (τ_f) along a possible décollement plane situated 20 m below the glacier-drift interface (values from Table 2). Due to subglacial permafrost (the Hättestrand (1997a) fracturing model, Fig. 15) pore-water pressure is zero and thus, according to these calculations, the shear strength is overrun by the shear stress only in the most marginal part (outer 1.5 km), which thus contradicts the formation of a fracturing zone.

The tectonic stress field beneath a glacier can be theoretically analysed to see if the 'fracturing model' is operational from a soil mechanics point of view. Fig. 16 shows a 10 km long cross-section of a glacier, deliberately chosen with a steep surface gradient to give best possible conditions for a high total glaciotectonic stress at the base. The stress field along the glacier/drift interface and a possible décollement surface along the drift/bedrock interface can be calculated from the following equations, all modified from Aber et al. (1989) and Benn and Evans (1998). Calculated stress and strength values are also shown in Table 2 for 1 km increments along the profile.

Deformation beneath the glacier can take place when the induced basal shear stress exceeds the strength of the subglacial material. According to Aber et al. (1989) the glacier induces two kinds of stresses on its bed, a *glaciostatic pressure* due to the static weight of the ice and a *glaciodynamic stress*—a drag or shear stress—due to movement of the glacier over its bed. The glaciostatic pressure at the ice/drift interface (σ_{zi}) is given by the equation

$$\sigma_{zi} = \rho_i g h_i \ (\mathrm{N/m^2}), \tag{1}$$

where ρ_i is ice density (900 kg/m^3), g the acceleration due to gravity (10 ms^{-2}) and h_i is the ice thickness (m). The same pressure is transferred downward to a possible décollement plane, with addition of the weight of the drift column, as a vertical normal stress σ_{zd} according to

$$\sigma_{zd} = \rho_i g h_i + \rho_d g h_d, \tag{2}$$

where ρ_d is the bulk density of drift and h_d the thickness of the drift sheet. The glaciostatic load is partly transferred to a horizontal stress (σ_x) that relates to

Table 2
Glaciostatic pressure at the ice/drift interface (σ_{zi}, Eq. (1)), vertical normal stress (σ_{zd}, Eq. (2)) at the drift/bedrock interface, horizontal stress (σ_x, Eq. (4)), cumulative lateral stress ($\sum\Delta\sigma_x$, Eq. (6)), shear stress (τ_b, Eq. (7)), total glaciotectonic stress (σ_{gt}, Eq. (8)) and shear strength (τ_f, Eq. (9)) at a possible décollement plane along the drift/bedrock interface, calculated for 1 km increments of the ice sheet profile, shown in Fig. 16

km	h_i (m)	σ_{zi} (kN/m^2) (1)	σ_{zd} (kN/m^2) (2)	σ_x (0.25σ_{zi}) (kN/m^2) (4)	$\Sigma\Delta\sigma_x$ (kN/m^2) (6)	α (deg)	τ_b (kN/m^2) (7)	σ_{gt} (kN/m^2) (8)	τ_f (kN/m^2) (9)
0	1000	9000	9400	2250	0				5427
1	980	8820	9220	2205	45	0.9	145	190	5323
2	950	8550	8950	2138	113	1.4	211	323	5167
3	910	8190	8590	2048	203	1.8	270	472	4959
4	860	7740	8140	1935	315	2.3	320	635	4700
5	795	7155	7555	1789	461	2.9	386	847	4362
6	710	6390	6790	1598	653	3.8	453	1105	3920
7	600	5400	5800	1350	900	5.0	500	1400	3349
8	450	4050	4450	1013	1238	6.8	523	1761	2569
9	250	2250	2650	563	1688	9.0	415	2102	1530
10	0	0	400	0	2250	11.3	78	2328	231

All stress values are in kN/m^2. Values, used in the calculations are: bulk density of drift (ρ_d) 2000 kg/m^3, internal angle of friction (ϕ) 30°, acceleration due to gravity (g) 10 ms^{-2}, depth of décollement plane beneath ice/drift interface 20 m. The calculated values for total glaciotectonic stress (σ_{gt}) and shear strength (τ_f) along the profile are shown graphically in Fig. 16.

the glaciostatic load (σ_{zi}) as

$$\sigma_x = [v/(1-v)]\sigma_{zi}, \quad (3)$$

where v is Poisson's ratio (for soft sediments and granular materials ca 0.2; van der Wateren, 1985). Eq. (3) can thus be rewritten as

$$\sigma_x = 0.25\sigma_{zi}. \quad (4)$$

The difference in ice thickness along the profile gives a gradually changing vertical load (σ_{zi}); thus there also is a change in the lateral stress component from point to point generating a lateral pressure gradient regardless of the direction or rate of ice movement. The difference in lateral stress between two points ($\Delta\sigma_x$) can be expressed as

$$\Delta\sigma_{x1/2} = \sigma_{x1} - \sigma_{x2} = 0.25\rho_i g(h_{i1} - h_{i2}). \quad (5)$$

Thus, the cumulative lateral stress ($\sum\Delta\sigma_x$), increasing towards the margin of the glacier, can be written as

$$\sum\Delta\sigma_x = \Delta\sigma_{x1/2} + \Delta\sigma_{x2/3} + \Delta\sigma_{x3/4} + \cdots. \quad (6)$$

This equation also shows that the lateral stress gradient becomes gradually steeper towards the margin with a higher rate of stress change along the flow line. According to Aber et al. (1989) the distance over which this lateral stress is built up is probably limited to 10 km or less behind the ice margin. To this lateral glaciostatic stress the glaciodynamic stress, induced by the ice movement into the subglacial bed, must be added.

The shear stress along the ice/bed interface or a possible décollement plane along the drift/bedrock interface (τ_b) can be calculated from:

$$\tau_b = \rho g h \sin\alpha; \quad \tau_b = \sigma_{zd}\sin\alpha, \quad (7)$$

where α is the angle of the glacier surface. The total glaciotectonic stress (σ_{gt}), induced into the subglacial drift sheet at any chosen point along the profile would thus be:

$$\sigma_{gt} = \Sigma\Delta\sigma_x + \tau_b. \quad (8)$$

A failure in the drift sheet could thus occur if the total glaciotectonic stress along any potential plane of failure exceeds the shear strength (τ_f) along that plane. The shear strength can be calculated from:

$$\tau_f = c + (\sigma_n - u)\tan\phi = c + \sigma'\tan\phi, \quad (9)$$

where c is the material cohesion (zero for frictional, unfrozen sediments), σ_n the normal total stress towards the plane of failure, u the pore-water pressure, σ' the effective normal stress ($\sigma_n - u$) and ϕ the internal angle of friction (for frictional sediments, ca 30°).

In the 'fracturing model', the ice sheet is frozen on to a frozen drift sheet up-ice of, but to some length also down-ice of the postulated fracturing zone (Fig. 15, time-slice boxes 2–3). Thus there is no basal melting producing melt-water, which in any case could not reach unfrozen bedrock or sediment beneath the subglacial permafrost, and we should not expect any high pressure-head of possible ground water in the bedrock or drift beneath the PCS. With a pore-water pressure (u) equal to zero, the effective normal stress (σ') will equal the total stress (σ_n), giving maximum shear strength (τ_f) along a potential décollement plane at the drift/bedrock interface. The calculated values of shear strength and total glaciotectonic stress (σ_{gt}) (Table 2), plotted in the lower panel of Fig. 16, show that shear strength is very much higher than any induced glaciotectonic stress along most parts of the profile, except for the outermost ca 1.5 km. These calculations thus show that a décollement plane can hardly form in the predicted fracturing zone, lying well back from the ice margin according to Hättestrand (1997a). Therefore fracturing of a frozen subglacial drift sheet is probably also unlikely.

Contrary to this, the proposed 'reshaping model' fits well with the calculated basal stress pattern in Fig. 16. As stated earlier there is clear evidence from the Indån valley that the reshaping of transverse ridges into Rogen moraines takes place in a near-marginal position. This would then be where the glacier has reached the pressure melting point, producing basal melt water which 'pumps up' a basal pore-water pressure and thus reduces the shear strength of the now unfrozen subglacial sediments. These sediments—and landforms—will, in a more localized pattern, fail and deform where induced shear stresses are larger than shear strength and the deformation time will be short and interrupted by deglaciation.

8.2.2. The geomorphological counter-evidence

The 'fracturing model' (Hättestrand, 1997a; Hättestrand and Kleman, 1999) implies an extension of a pre-existing drift sheet; for the type locality in the Rogen area they give extension values of 35–60% of such a drift sheet. If we take a glacier as an analogue, transverse crevasses may develop on the surface due to extending flow. These crevasses will, however, heal in a down-flow direction when extension is replaced by compression or, if extension should continue to the glacier margin, disappear due to melting of the glacier. If we now transfer this analogue into the subglacial environment with, in the proximal direction, a frozen drift sheet there would be two possible scenarios, on condition that the 'fracturing model' works on a soil-mechanics basis.

The first scenario is that the fracturing zone with extension would act as a conveyer belt of frozen sediments in the ice-flow direction, the sediments gradually loosing their frozen state and, when coming into the marginal compressive zone forming a gradually thickening sub-marginal till wedge (i.e. Boulton, 1996a, b) or a marginal compressive belt (van der Wateren, 1995). However, such features have never been described delimiting the distal end of coherent Rogen/ribbed moraine tracts.

The second scenario is that the fracturing zone distally transforms into a wide subglacial deforming bed zone where more or less total remoulding and spread-out deposition of the drift sheet sediments under wet-based conditions occurs before they reach the ice-marginal zone. However, the Indån Rogen moraines indicate a late-stage and near-marginal deformation. There would thus not be much space for development of a distal deforming-bed zone that could effectively distribute excess material from a fracturing zone.

9. Final conclusions and remarks

- Recent mapping approaches of Rogen/ribbed moraine areas give valuable information on large-scale spatial distribution of these landforms and give us understanding of paleoflow patterns at an ice sheet-scale.
- However, at this scale it is also evident that genetically very different moraines are included into the ribbed moraine concept, e.g. the typically developed Swedish Rogen moraine *vs*. the 'Irish' large-scale ribbed moraine, and the very wide spectra of landforms put into the Hättestrand's (1997b) ribbed moraine concept. Used in this manner, ribbed moraine must be considered as a polygenetic group of landforms.
- The more precise landform-generating processes cannot be deciphered from a 'birds eye view'; these can only be concluded in combination with field-based, detailed studies on sediment facies and architecture and possibly occurring glaciotectonics.
- Gathered field data in this study support that Rogen moraine ridges (sensu stricto) are the reshaped remains of pre-existing moraine ridges, precursor ridges.
- In the investigation area these precursor ridges were dominantly built up by stacked sequences of debris-flow deposits, but such ridges can probably be formed by a number of different processes and in a number of different deglacial environments.
- It is proposed that the primary and in situ landform build-up was prior to the last deglaciation of the area—presumably during Early Weichselian deglaciation of a west-centred Scandinavian ice sheet (cf. Kleman et al., 1997). Frozen-bed conditions of the interior part of the succeeding LGM Scandinavian ice sheet give an explanation to the preservation of the relict, precursor landforms prior to the variable re-moulding of these into Rogen moraine during wet-based conditions in the marginal area during deglaciation.
- The validity of the 'fracturing model' (Hättestrand, 1997a) as responsible for Rogen moraine formation—in addition to the more theoretical objections on basis of soil mechanics and geomorphological consequences—is not supported by field data from the present study.

Acknowledgements

Funds used for this work was provided by the Faculty of Science, Lund university. Field assistance was given by my oldest son Henrik, and my youngest son Nicklas drew Fig. 13. Thanks go to my dear boys! Lars Hinders, Vårmhus, and Korsnäs AB, Orsa, are thanked for permission to excavate the Eggling and Kipholstjärnen sites, respectively. Svante Björck, Christian Hjort, Kurt H. Kjær and Mark Johnson gave valuable comments and suggestions for improvements on the original manuscript. QSR reviewers Dave Evans and Dave Roberts really made a difference in strengthening this paper.

References

Aario, R., 1987. Drumlins of Kuusamo and Rogen-ridges of Rauna, northeastern Finland. In: Menzies, J., Rose, J. (Eds.), Drumlin Symposium. A.A. Balkema, Rotterdam, pp. 87–101.

Aber, J.S., Croot, D.G., Fenton, M.M., 1989. Glaciotectonic Landforms and Structures. Kluwer Academic Publishers, Dortrecht 200pp.

Alley, R.B., 1992. How can low-pressure channels and deforming tills coexist subglacially? Journal of Glaciology 38, 200–207.

Aylsworth, J.M., Shilts, W.W., 1989. Bedforms of the Keewatin Ice Sheet, Canada. Sedimentary Geology 62, 407–428.

Benn, D.I., 1992. The genesis and significance of 'hummocky moraine': evidence from the Isles of Skye, Scotland. Quaternary Science Reviews 11, 781–799.

Benn, D.I., 1994. Fabric shape and the interpretation of sedimentary fabric data. Journal of Sedimentary Research A 64 (4), 910–915.

Benn, D.I., Evans, D.J.A., 1996. The interpretation and classification of subglacially-deformed materials. Quaternary Science Reviews 15, 23–52.

Benn, D.I., Evans, D.J.A., 1998. Glaciers and Glaciation. Arnold, London 734pp.

Bennett, M.R., Boulton, G.S., 1993. A reinterpretation of Scottish 'hummocky moraine' and its significance for the deglaciation of the Scottish Highlands during the Younger Dryas or Loch Lomond Stadial. Geological Magazine 130, 301–318.

Björck, S., Möller, P., 1987. Late Weichselian environmental history in southeastern Sweden during the deglaciation of the Scandinavian ice sheet. Quaternary Research 28, 1–37.

Björck, S., Kromer, B., Johnsen, S., Bennike, O., Hammarlund, D., Lemdahl, G., Possnert, G., Rasmussen, T.L., Wohlfarth, B., Hammer, C.U., Spurk, M., 1996. Synchronized terrestrial-atmospheric deglacial records around the North Atlantic. Science 274, 1150–1160.

Borgström, I., 1999. Basal ice temperatures during late Weichselian deglaciation: comparison of landform assemblages in west-central Sweden. Annals of Glaciology 28, 9–15.

Bouchard, M.A., 1989. Subglacial landforms and deposits in central and northern Québec, Canada, with emphasis on Rogen moraines. Sedimentary Geology 62, 293–308.

Boulton, G.S., 1972. Modern arctic glaciers as depositional models for former ice sheets. Geological Society of London Quarterly Journal 128, 361–393.

Boulton, G.S., 1987. A theory of drumlin formation by subglacial sediment deformation. In: Menzies, J., Rose, J. (Eds.), Drumlin Symposium. A.A. Balkema, Rotterdam, pp. 25–80.

Boulton, G.S., 1996a. Theory of glacial erosion, transport and deposition as a consequence of subglacial sediment deformation. Journal of Glaciology 42, 43–62.

Boulton, G.S., 1996b. The origin of till sequences by subglacial sediment deformation beneath mid-latitude ice sheets. Annals of Glaciology 22, 75–84.

Cato, I., 1987. On the definitive connection of the Swedish time Scale with the present. Sveriges Geologiska Undersökning Ca 68, 55pp.

Clark, C.D., 1994. Large-scale ice-moulding: a discussion of genesis and glaciological significance. Sedimentary Geology 91, 253–268.

Clark, P.U., 1991. Striated clast pavements: products of deforming subglacial sediments? Geology 19, 530–533.

Clark, C.D., Meehan, R.T., 2001. Subglacial bedform geomorphology of the Irish Ice Sheet reveals major configuration changes during growth and decay. Journal of Quaternary Science 16, 483–496.

Clark, P.U., Walder, J.S., 1994. Subglacial drainage, eskers, and deforming beds beneath the Laurentide and Eurasian ice sheets. Geological Society of America Bulletin 106, 304–314.

Cobbold, P.R., Quinquis, H., 1980. Development of sheath folds in shear regimes. Journal of Structural Geology 2, 119–126.

Cowan, W.R., 1968. Ribbed moraine: till-fabric analysis and origin. Canadian Journal of Earth Sciences 5, 1145–1159.

Dowdeswell, J.A., Sharp, M.J., 1986. Characterization of pebble fabrics in modern terrestrial glacigenic sediments. Sedimentology 33, 699–710.

Edwards, M., 1986. Glacial environments. In: Reading, H.G. (Ed.), Sedimentary Environments and Facies. Blackwell Scientific Publications, Oxford, pp. 445–470.

Eyles, N., 1979. Facies of supraglacial sedimentation on Islandic and Alpine temperate glaciers. Canadian Journal of Earth Science 16, 1341–1361.

Eyles, N., 1983. Modern Icelandic glaciers as depositional models for 'hummocky moraine' in the Scottish Highlands. In: Evensson, E.B., Schlüchter, Ch., Rabassa, J. (Eds.), Tills & Related Deposits. A.A. Balkema, Rotterdam, pp. 47–59.

Eyles, N., Eyles, C.H., Miall, A.D., 1983. Lithofacies types and vertical profile models; an alternative approach to the description and environmental interpretation of glacial diamict and diamictite sequences. Sedimentology 30, 393–410.

Fromm, E., 1991. Varve chronology and deglaciation in south-eastern Dalarna, Central Sweden. Sveriges Geologiska Undersökning Ca 77, 49pp.

Frödin, G., 1925. Studien über die Eisscheide in Zentral-skandinavien. Bulletin of the Geological Institution, University of Uppsala 19, 129–214.

Granlund, E., 1943. Beskrivning till jordartskarta över Västerbottens län nedanför odlingsgränsen. Sveriges Geologiska Undersökning Ca 26, 165pp. (in Swedish).

Hart, J.K., Boulton, G.S., 1991. The interrelation of glaciotectonic and glaciodepositional processes within the glacial environment. Quaternary Science Reviews 10, 335–350.

Hättestrand, C., 1994. Boulder pavements in central Sweden–remnants of a pre-late Weichselian landscape? Geografiska Annaler 76A, 153–160.

Hättestrand, C., 1997a. Ribbed moraines in Sweden—distribution pattern and palaeoglaciological implications. Sedimentary Geology 111, 41–56.

Hättestrand, C., 1997b. The glacial geomorphology of central and northern Sweden. Sveriges Geologiska Undersökning Ca 85, 47pp.

Hättestrand, C., Kleman, J., 1999. Ribbed moraine formation. Quaternary Science Reviews 18, 43–61.

Hicock, S.R., 1991. On subglacial stone pavements in till. Journal of Geology 99, 607–619.

Hjelmqvist, S., 1966. Beskrivning till berggrundskarta över Kopparbergs län. Sveriges Geologiska Undersökning Ca 40, 217pp. (in Swedish).

Hoppe, G., 1959. Glacial morphology and inland ice recession in northern Sweden. Geografiska Annaler 41A, 193–212.

Hughes, O.L., 1964. Surficial geology, Nichicun-Kaniapiskau map-area, Quebec. Geological Survey of Canada Bulletin 106, 20pp.

Kjær, K.H., Krüger, J., 2001. The final phase of dead-ice moraine development: processes and sediment architecture, Kötlujökul, Iceland. Sedimentology 48, 935–952.

Kleman, J., 1990. On the use of glacial striae for reconstruction of paleo-ice flow patterns—with application to the Scandinavian ice sheet. Geografiska Annaler 72A, 217–236.

Kleman, J., 1992. The palimpsest glacial landscape in northern Sweden—Late Weichselian deglaciation landforms and traces of older west-centered ice sheets. Geografiska Annaler 72A, 305–325.

Kleman, J., 1994. Preservation of landforms under ice sheets and ice caps. Geomorphology 9, 19–32.

Kleman, J., Borgström, I., 1990. The boulder fields on Mt Fulufjället, west-central Sweden—Late Weichselian boulder blankets and interstadial periglacial phenomena. Geografiska Annaler 72A, 63–78.

Kleman, J., Borgström, I., 1996. Reconstruction of palaeo-ice sheets—the use of geomorphological data. Earth Surface Processes and Landforms 21, 893–909.

Kleman, J., Hättestrand, C., 1999. Frozen-bed Fennoscandian and Laurentide ice sheets during the Last Glacial maximum. Nature 402, 63–66.

Kleman, J., Borgström, I., Robertsson, A.-M., Liljesköld, M., 1992. Morphology and stratigraphy from several deglaciation events in the Transtrand mountains, western Sweden. Journal of Quaternary Science 7, 1–16.

Kleman, J., Hättestrand, C., Borgström, I., Stroeven, A., 1997. Fennoscandian palaeoglaciology reconstructed using a glacial geological inversion model. Journal of Glaciology 43, 283–299.

Kleman, J., Hättestrand, C., Clarhäll, A., 1999. Zooming in on frozen-bed patches: scale-dependent controls on Fennoscandian ice sheet basal thermal zonation. Annals of Glaciology 28, 189–194.

Knight, J., McCabe, A.M., 1997. Identification and significance of ice-flow-transverse subglacial ridges (Rogen moraines) in northern Ireland. Journal of Quaternary Science 12, 519–524.

Knight, J., McCarron, S.G., McCabe, A.M., 1999. Landform modification by paleo-ice streams in east-central Ireland. Annals of Glaciology 28, 161–167.

Krüger, J., Kjær, K.H., 1999. De-icing progression of ice-cored moraine in a humid, subpolar climate, Kötlujökul, Iceland. Holocene 10, 721–731.

Kurimo, H., 1980. Depositional deglaciation forms as indicators of different glacial and glaciomarginal environments. Boreas 9, 179–191.

Lagerbäck, R., 1988a. The Veiki moraines in northern Sweden—widespread evidence of an Early Weichselian deglaciation. Boreas 17, 469–486.

Lagerbäck, R., 1988b. Periglacial phenomena in the wooded areas of north Sweden—relicts from the Tärendö interstadial. Boreas 17, 487–499.

Lagerbäck, R., Robertsson, A.-M., 1988. Kettle holes—stratigraphic archives for Weichselian geology and palaeoenvironment in northernmost Sweden. Boreas 17, 439–468.

Larsen, N.K., Piotrowski, J.A., 2003. Fabric pattern in a basal till succession and its significance for reconstructing subglacial processes. Journal of Sedimentary Research 73, 725–734.

Lawson, D.E., 1979. Sedimentological analysis of the western terminus region of the Matanuska Glacier, Alaska. Report 79-9, Cold Regions Research and Engineering Laboratory (CRREL), Hanover, NH, 96pp.

Lawson, D.E., 1981. Sedimentological characteristics and classification of depositional processes and deposits in the glacial environment. Report 81-27, Cold Regions Research and Engineering Laboratory (CRREL), Hanover, NH, 16pp.

Lawson, D.E., 1982. Mobilization, movement and deposition of subaerial sediment flows, Matanuska Glacier, Alaska. Journal of Geology 90, 279–300.

Lawson, D.E., 1988. Glacigenic resedimentation: classification concepts and application to mass-movement processes and deposits. In: Goldthwait, R.P., Matsch, C.L. (Eds.), Genetic Classification of Glacigenic Deposits. A.A. Balkema, Rotterdam, pp. 147–169.

Lundqvist, G., 1943. Norrlands jordarter. Sveriges Geologiska Undersökning C 457, 166pp. (in Swedish).

Lundqvist, J., 1958. Beskrivning till jordartskarta över Värmlands län. Sveriges Geologiska Undersökning Ca 38, 229pp. (in Swedish).

Lundqvist, J., 1969. Problems of the so-called Rogen moraine. Sveriges Geologiska Undersökning C 648, 32pp.

Lundqvist, J., 1981. Moraine morphology. Terminological remarks and regional aspects. Geografiska Annaler 63A, 127–137.

Lundqvist, J., 1989. Rogen (ribbed) moraine—identification and possible origin. Sedimentary Geology 62, 127–138.

Lundqvist, J., 1997. Rogen moraine—an example of two-step formation of glacial landscapes. Sedimentary Geology 111, 27–40.

Mark, D.M., 1973. Analysis of axial orientation data, including till fabrics. Geological Society of America Bulletin 84, 1369–1374.

McCabe, A.M., Knight, J., McCarron, S.G., 1998. Evidence for Heinrich event 1 in the Britich Isles. Journal of Quaternary Science 13, 549–568.

McCabe, A.M., Knight, J., McCarron, S.G., 1999. Ice-flow stages and glacial bedforms in north central Ireland: a record of rapid environmental change during the last termination. Journal of the Geological Society, London 156, 63–72.

Menzies, J., Shilts, W.W., 1996. Subglacial environments. In: Menzies, J. (Ed.), Past Glacial Environments—Sediments, Forms and Techniques. Glacial Environments, vol. 2. Butterworth-Heineman, Oxford, pp. 15–136.

Möller, P., 1987. Moraine morphology, till genesis, and deglaciation pattern in the Åsnen area, south-central Småland, Sweden. LUNDQUA Thesis 20, Department of Quaternary Geology, Lund University, 146pp.

Nordell, P.O., 1984. Dokumentation av istida landformer, isavsmältning och högsta kustlinje i Våmådalen och Orsasjöns randområden. Information från länsstyrelsen i Kopparbergs län, Naturvårdsenheten, N 4, 133pp. (in Swedish).

Paul, M.A., 1983. The supraglacial landsystem. In: Eyles, N. (Ed.), Glacial Geology. An Introduction for Engineers and Earth Scientists. Pergamon Press, Oxford, pp. 71–90.

Paul, M.A., Eyles, N., 1990. Constraints on the preservation of diamict facies (melt-out tills) at the margins of stagnant glaciers. Quaternary Science Reviews 9, 51–69.

Piotrowski, J.A., Kraus, A., 1997. Response of sediment to ice sheet loading in northwestern Germany: effective stresses and glacier bed stability. Journal of Glaciology 43, 495–502.

Piotrowski, J.A., Larsen, N.K., Junge, F.W., 2004. Reflections on soft beds as a mosaic of deforming and stable spots. Quaternary Science Reviews 23, 993–1000.

Shaw, J., 1979. Genesis of the Sveg till and Rogen moraines of central Sweden: a model of basal melt out. Boreas 8, 409–426.

Shaw, J., 1982. Melt-out till in the Edmonton area, Alberta, Canada. Canadian Journal of Earth Science 19, 1548–1669.

Shaw, J., 1983. Forms associated with boulders in melt-out till. In: Evenson, E.B., Schluchter, Ch., Rabassa, J. (Eds.), Tills and Related Deposits: Genesis, Petrology, Application, Stratigraphy. A.A. Balkema, Rotterdam, pp. 3–12.

Sugden, D.E., John, B.S., 1976. Glaciers and Landscape. Edward Arnold Publishers, London, 376pp.

van der Wateren, F.M., 1985. A model of glacial tectonics, applied to the ice-pushed ridges in central Netherlands. Bulletin of the Geological Society of Denmark 34, 55–74.

van der Wateren, F.M., 1995. Processes of glaciotectonism. In: Menzies, J. (Ed.), Modern Glacial Environments—Processes, Dynamics and Sediments. Glacial Environments, vol. 1. Butterworth-Heineman, Oxford, pp. 309–335.

van der Wateren, F.M., Kluiving, S.J., Bartek, L.R., 2000. Kinematic indicators of subglacial shearing. In: Maltman, A.J., Hubbard, B., Hambrey, M.J. (Eds.), Deformation of Glacial Materials. Geological Society of London Special Publications 176, pp. 259–278.

Walder, J.S., Fowler, A., 1994. Channelized subglacial drainage over a deformable bed. Journal of Glaciology 40, 199–200.

Wohlfarth, B., 1996. The chronology of the Last Termination: a review of radiocarbon-dated, high-resolution terrestrial stratigraphies. Quaternary Science Reviews 15, 267–284.